THE ACTIVATION OF HYDROGEN PEROXIDE AND DIOXYGEN FOR THE OXIDATION OF ORGANIC COMPOUNDS

BY

CHENG XU

A DISSERTATION PRESENTED TO THE GRADUATE SCHOOL
OF THE UNIVERSITY OF FLORIDA IN PARTIAL FULFILLMENT
OF THE REQUIREMENTS FOR THE DEGREE OF
DOCTOR OF PHILOSOPHY

UNIVERSITY OF FLORIDA

1999

ACKNOWLEDGMENTS

It was a long journey for me through graduate school I stopped several times, and thought about giving up But finally, I am accomplishing my goal

There are numerous people who have helped me along my journey First I would like to thank my late research director, Dr Russell S Drago, for his encouragement and patience He was my mentor It was he who told me how to practice chemistry and his influence will be with me throughout my whole scientific career

I would also like to give my special thanks to my adviser Dr David E Richardson His support and guidance helped me continue through the difficult period after the loss of my former adviser, Dr Drago

My peers have been very supportive Every former Drago group member and current Richardson group member has given me unlimited help during my time at the University of Florida. These names are important for me to remember They are Dr Ken Lo, Dr Alfredo Mateus, Ben Gordon, Karen Frank, Dr John Osegovic, Dr Edwin Webster, Dr Michael Robbins, Jake Oyloe, Dr Huarong Yao Joy Mendez, and Celeste Regino

My wife, Hong Wu, is the driving force that pushes me all the time My beautiful daughter, Catherine H Xu, is an inspiration for doing my research work

I give my sincere thanks to my mother, Zhenhua Tao and my father, Junxuan Xu. Mom and Dad this dissertation is also dedicated to you both

Finally, I would like to thank Dr. Daniel Talham, Dr. William Dolbier, Dr. Martin Vala, Dr. Hai Ping Cheng, and Dr. Michael Scott for the help they offered during these years.

TABLE OF CONTENTS

ACKNOWLEDGMENTS ii

ABSTRACT vi

CHAPTERS

1 INTRODUCTION TO THE CATALYTIC OXIDATION OF ORGANIC COMPOUND 1

Application of Homogeneous Oxidation Catalysis in Industry 2
Activation of Dioxygen 5
Activation of Dioxygen through Metal-Bound O_2 Intermediate 7
Oxidation Reation in Biological System 9
Kinetics of O_2 Oxidation Reaction 10
Activation of Alkyl Hydroperoxide and Hydrogen Peroxide 11
Catalytic Epoxidation of Olefins 13
Selective Catalytic Oxidation of Saturated Hydrocarbons 16
Conclusions 18

2 SINGLE STEP SYNTHESIS OF SOLID ADIPIC ACID BY CATALYTIC OXIDATION OF CYCLOHEXANE IN AIR 20

Introduction 20
Experimental 28
Results and Discussion 31
Conclusions 44

3 ACTIVATION OF HYDROGEN PEROXIDE BY MIXED LIGAND IRON (III) COMPLEXES FOR THE SELECTIVE OXIDATION OF HYDROCARBONS 45

Introduction 45
Experimental 50
Results and Discussion 53
Conclusions 64

4 ENANTIOSELECTIVE EPOXIDATION CATALYZED BY MANGANESE SCHIFF BASE COMPLEXES 65

Introduction 65
Experimental 73
Results and Discussion 77
Conclusions 87

5 OXIDATION OF MUSTARD SIMULANTS CATALYZED BY BICARBONATE SALTS 89

Introduction 89
Experimental 95
Results and Discussion 96
Conclusions 100

6 ACTIVATION OF HYDROGEN PEROXIDE IN BASIC AQUEOUS SOLUTION BY COPPER(II) WITH 2-PYRIDYL ACETIC ACID 102

Introduction 102
Experimental 104
Results and Discussion 108
Conclusions 116

REFERENCES 118

BIOGRAPHICAL SKETCH 126

Abstract of Dissertation Presented to the Graduate School
of the University of Florida in Partial Fulfillment of the
Requirements for the Degree of Doctor of Philosophy

THE ACTIVATION OF HYDROGEN PEROXIDE AND DIOXYGEN FOR THE OXIDATION OF ORGANIC COMPOUNDS

By

Cheng Xu

August 1999

Chairman: David E. Richardson
Major Department: Chemistry

Adipic acid is used for the manufacture of nylon 6,6. The industrial adipic acid process uses nitric acid as the oxidant, which causes environmental problems.

Our research demonstrates that some iron and ruthenium complexes catalyze the oxidation of cyclohexane to adipic acid using air as the oxidant. This process may offer an environmentally friendly way for adipic acid synthesis.

Great progress has been made for the hydrocarbon oxidation by the Gif system. We improved the well-established Gif system by increasing the reaction efficiency and the life-time of the catalyst.

Several iron (III) complexes were synthesized. [Fe^{III} (DPA)(Phen)ClO$_4$] complex is the most efficent catalyst and at least 70% more active than the best catalyst in the literature. Evidence indicates the reaction is occurring via a non-radical mechanism. An iron (III)-peroxo intermediate was also isolated.

Chiral epoxides are important building blocks in the synthesis of natural products. We synthesized new types of chiral manganese complexes derived from amino acids. Enantioselective styrene epoxidations using bulky manganese complexes introduce ee values of 15%.

The safety and environmental impact of the destruction of chemical warfare agents are of great concern to the public. Our laboratory has shown the excellent catalytic oxidation of EtPhS by formation of the strong oxidant peroxymonocarbonate. However, the limited solubility of $NaHCO_3$ has restricted the further enhancement of the catalytic ability of this novel oxidation system.

A modified system has been established by our work. By using NH_4HCO_4 as catalyst and C_2H_5OH/H_2O as the solvent, the reaction rate for the oxidation of EtPhS can be increased 10 times compared with the original system, and using a new bicarbonate salt with a large organic cation further increases the reaction rate.

A large number of patents address the goal of replacing hypochlorite-containing bleaches. We showed that in basic aqueous solution $CuCl_2$ and 2-pyridylacetic acid form a complex that is unusually active for the oxidation of organic substrates using H_2O_2. The maximum concentration of the active species occurs when the ratio of ligand to metal is 8:1. Several copper (II) complexes can be isolated from solution. The isolated complexes require excess ligand for full catalytic efficiency.

CHAPTER 1
INTRODUCTION TO THE CATALYTIC OXIDATION OF ORGANIC COMPOUNDS

The general definition of oxidation in organic chemistry is either the elimination of hydrogen or the replacement of a hydrogen atom bonded to carbon with another more electronegative element such as oxygen. The common functional group transformations involved in oxidation reactions are: (1) oxidation of alcohols to aldehydes, ketones, or carboxylic acids, (2) epoxidation of alkenes to form epoxides; (3) oxidative cleavage at functional groups such as carbon-carbon double bonds, (4) oxidation of ketones and aldehydes, (5) allylic oxidation of olefins, and (6) oxidation of saturated hydrocarbons. The catalytic oxidation chemistry considered in this dissertation is mainly oxygen transfer reactions from oxidant to an organic molecule.

In general, oxidants have been grouped into three classes: oxygen, ozone, and peroxides; transition-metal derivatives, such as permanganate ion, chromic acid and ruthenium tetroxide; and other oxidizing agents, such as selenium dioxide and peracids.

A typical example of using traditional oxidants is the well-known *Baeyer-Villiger* oxidation reaction.[1] In the presence of acid catalysts, peracids oxidize carbonyl compounds by inserting an oxygen atom into one of the carbon-carbon bonds at the carbonyl group (Figure 1.1).

The subject of catalytic oxidation usually includes three traditionally areas: homogeneous, heterogeneous and biochemical enzymatic oxidation. In this chapter, the only focus was on the catalytic homogeneous oxidation. Selective oxidation processes, in which hydrocarbon molecules are oxygenated to form alcohols, aldehydes or acids, are the basis of the modern petrochemical industry and constitute the largest category of catalytic organic reactions. Practically, processes including catalytic oxidation reactions obtain most monomers used in manufacturing of artificial fiber and plastic.[2]

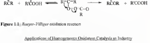

Figure 1.1 *Baeyer-Villiger* oxidation reaction

Applications of Homogeneous Oxidation Catalysis in Industry

Catalytic oxidation reactions can be traced back to 1820, when Davy[3] showed that ethanol is oxidized to acetic acid in the presence of platinum (Equation 1.1).

$$CH_3CH_2OH + O_2 \xrightarrow{Pt} CH_3CO_2H + H_2O \quad (1.1)$$

The Wacker process, which is used for the production of acetaldehyde from ethylene, is the first industrial applications of homogeneous oxidation.[4] The oxidation is catalyzed with cupric chloride and palladium chloride and air or oxygen is used as oxidant (Equation 1.2-1.5).

Vinyl acetate can be produced from ethylene and acetic acid by using same type of catalyst (Equation 1.6).[5]

$$CH_2{=}CH_2 + H_2O + PdCl_2 \longrightarrow CH_3CHO + Pd + 2\,HCl \qquad (1.2)$$

$$Pd + 2\,CuCl_2 \longrightarrow PdCl_2 + 2\,CuCl \qquad (1.3)$$

$$2\,CuCl + 1/2\,O_2 + 2\,HCl \longrightarrow 2\,CuCl_2 + H_2O \qquad (1.4)$$

$$CH_2{=}CH_2 + 1/2\,O_2 \xrightarrow{Pd\,(II),\ Cu\,(II)} CH_3CHO \qquad (1.5)$$

$$CH_2{=}CH_2 + CH_3COOH + 1/2\,O_2 \xrightarrow{Pd\,(II)} CH_2{=}CHOCOCH_3 \qquad (1.6)$$

The production of terephthalic acid, which is used to make polyester fibers, is the largest commercial homogeneous catalytic oxidation. Terephthalic acid is obtained by the oxidation of *p*-xylene with air using soluble cobalt acetate or manganese acetate as catalysts. Metal bromides are often used as a "promoter" for the oxidation of *p*-xylene to terephthalic acid.[6] Some applications of homogeneous oxidation catalysis to the chemical industry are summarized in Table 1.1.

The use of classical oxidants for oxidation reaction leads to a big environmental problem, because of the generation of numerous amounts of byproducts. For example, one mole of $Pb(OAc)_4$ (OAc = acetate) as oxidant will form one mole of $Pb(OAc)_2$ and two moles of acetic acid when oxidizing carbon carbon bonds (Figure 1.2).[7] Recently, more attention has been paid in the use of dioxygen (or air) and hydrogen peroxide as oxidants which are inexpensive and environmentally friendly

Table 1.1. Major applications of homogeneous oxidation catalysis in industry [5]

$$CH_2{=}CH_2 + 1/2\ O_2 \xrightarrow{PdCl_2,\ CuCl} CH_3CHO$$

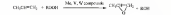

$$CH_3CH{=}CH_2 + ROOH \xrightarrow{\text{Mo, V, W compounds}} CH_3CH{-}CH_2\ (\text{epoxide, } O) + ROH$$

$$c\text{-}C_6H_{12} \xrightarrow[\text{Co salts}]{O_2} c\text{-}C_6H_{11}OH + c\text{-}C_6H_{10}O \xrightarrow{HNO_3} \text{adipic acid}$$

$$p\text{-xylene} + O_2 \xrightarrow{\text{Co salts}} \text{terephthalic acid and esters}$$

$$n\text{-}C_4H_{10} + O_2 \xrightarrow{\text{Cr, Mn, Co, Ni salts}} 2\ CH_3COOH$$

$$C_6H_5CO_2H + O_2 \xrightarrow{\text{Cu(II) benzoate / Mg(II) benzoate}} C_6H_5OH + CO_2$$

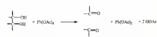

Figure 1.2: Oxidative cleavage of carbon-carbon bonds by using $Pb(OAc)_4$

Activation of Dioxygen

The molecular orbital configuration of O_2 is $1\sigma_g^2\ 1\sigma_u^2\ 2\sigma_g^2\ 2\sigma_u^2\ 3\sigma_g^2\ 1\pi_u^4\ 1\pi_g^2$. Although the oxidation of organic substrates by dioxygen is exothermic, the triplet electronic character of the ground state of dioxygen inhibits its reactivity with the organic compounds, which are singlets by the spin conservation rule. In principle, the reduction potential for O_2 / H_2O couple $E^\circ = 1.23V$ (vs NHE) shows that dioxygen is a strong four electron oxidant (Equation 1.7)

$$O_2 + 4H^+ + 4e \longrightarrow 2H_2O \qquad (1.7)$$

In oxidation reaction, organic substrate only can provide one electron or one hydrogen atom per molecule, while dioxygen is a poor oxidant for one electron oxidation (O_2 / HO_2 couple $E^\circ = -0.10V$ vs NHE) (Figure 1.3). This accounts for the kinetic inactivity of dioxygen molecule

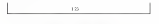

Figure 1.3 O_2 Reduction potentials vs NHE ($a_{H^+} = 1$)[9]

Activation of Dioxygen by Formation of Free Radical

Hydrocarbon molecules can be activated by abstraction of hydrogen resulting in the formation of free radicals, which then participate in a chain reaction. The presence of transition metal catalysts may accelerate the generation of radicals in liquid phase due to the reaction in Equation 1.8.

$$RCH_3 + M^{n+} \rightarrow RCH_2\bullet + H^+ + M^{(n-1)+} \qquad (1.8)$$

The alkyl radical interacts with dioxygen dissolved from the gas phase to form peroxy radicals (Equation 1.9)

$$RCH_2\bullet + O_2 \rightarrow RCH_2O_2\bullet \qquad (1.9)$$

Peracids, acids, aldehydes and carbon oxides are produced as a result of chain radical reactions. These O_2 oxidation processes are called autoxidation and are responsible for the degradation of many organic materials such as plastics, rubber, fibers, lubricating oils and fats, etc. The facility of electron transfer from hydrocarbon molecules to the metal producing the cation radical is related to the ionization potential of the organic substrate and the oxidizing power of the metal cation. Although initial studies were concerned mainly with finding ways of preventing autoxidation, it was soon recognized that the controlled autoxidation of hydrocarbons could be a useful method for preparing a wide range of oxygenated derivatives of hydrocarbons. The conversion of cumene to phenol and acetone, which was discovered by Hock and Lang in 1944,[10] is a well-known commercial autoxidation (Figure 1.4). Autoxidation becomes more complicated at high conversions of the substrate owing to the accumulation of secondary products, such as the easily oxidized aldehydes and ketones. Thus, low conversions (< 20%) are restricted for autoxidation syntheses, and excess unreacted substrate has to be recycled.

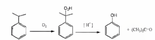

Figure 1.4. Transformation of cumene to phenol by autoxidation.

Activation of Dioxygen through Metal-Bound O_2 Intermediate

The spin barrier in dioxygen oxidation may be overcome by forming adduct of dioxygen with a metal complex. The frontier orbitals of the oxygen molecule in the ground state $^3\Sigma_g$ are doubly degenerate singly occupied, antibonding π_g^* orbitals. Usually such singly occupied orbitals have both electron acceptor and electron donor properties. When a transition metal has the appropriate energy and occupancy, a metal-O_2 complex is formed by electron transformation from the antibonding π_g^* orbital of dioxygen onto the empty d-orbital of the metal atom. An example of Co(II) complex activates dioxygen is shown in Figure 1.5.

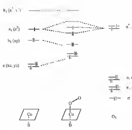

Figure 1.5: The spin pairing model for bonding O_2 to Co(II) complexes.[11]

The interaction of dioxygen with metal complexes can lead to the formation of a series of metal superoxo, peroxo, and oxo complexes (Equation 1.10):

$$M \xrightarrow{+O_2} \underset{\text{superoxo}}{MO_2} \xrightarrow{+M} \underset{\mu\text{-peroxo}}{MO_2M} \longrightarrow \underset{\text{oxo}}{2\,MO} \xrightarrow{+M} \underset{\mu\text{-oxo}}{MOM} \quad (1.10)$$

Oxidation Reaction in Biological System

Nature has its unique way for doing selective O_2 oxidation, which is accomplished by certain enzymatic systems. Some enzymes of the mono- and dioxygenase types incorporate one or both oxygen atoms of O_2 respectively into a substrate. A well-known monooxygenase is iron porphyrin-based cytochrome P-450. The key steps in the catalytic cycle is reductive activation of O_2, whereby one oxygen atom is reduced to H_2O and the other oxygen atom becomes available to form a high-valent iron-oxo species for the oxidation process (Figure 1.6).

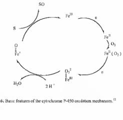

Figure 1.6: Basic features of the cytochrome P-450 oxidation mechanism.[12]

Kinetics of O_2 Oxidation Reaction

A general mechanism of O_2 oxidation reaction catalyzed by metal complexes can be illustrated in following set of equations (Equation 1.11 – 1.14).

$$\text{Cat} + O_2 \longrightarrow \text{Cat-}O_2 \qquad (1.11)$$

$$\text{Cat-}O_2 + \text{S} \underset{k_{-1}}{\overset{k_1}{\rightleftharpoons}} \text{Cat-}O_2\text{-S} \qquad (1.12)$$

$$\text{Cat-}O_2\text{-S} \xrightarrow{k_2} \text{Cat-O} + \text{P} \qquad (1.13)$$

$$\text{Cat-O} + \text{Red} \longrightarrow \text{Cat} + H_2O \qquad (1.14)$$

The key step of catalytic O_2 oxidation is dioxygen and substrate coordinating at the same metal on two adjacent sites. The substrate is then inserted into a metal-oxygen bond forming a peroxo metallocycle. The latter decomposes to the oxygenated substrate and oxo metal complex. In order to close the catalytic cycle, a co-reducing agent is required to reduce the oxo metal complex to the initial metal state. This co-reducing agent can be a hydrogen donor, water being produced in the course of the reaction, or the substrate itself, which would be oxidized.

The rate of formation of the product can be expressed by Equation 1.15, which is deduced from Equation 1.11-1.14. The expression equation for depicting the rate formation of homogeneous catalytic oxidation reactions (Equation 1.15) has the same form of the Michaelis – Menten equation, which is originally used to describe the rate of reaction in enzymatic systems.[13] K_M is called the Michaelis constant.

$$v = \frac{k_2 [\mathrm{Cat}]_0 [S]}{(k_{-1} + k_2) / k_1 + [S]} = \frac{k_2 [\mathrm{Cat}]_0 [S]}{K_M + [S]} \qquad (1.15)$$

Instead of using the co-reducing agent in situ in the reaction mixture, dioxygen may be reduced in a separate operation to form molecules such as hydrogen peroxide, sodium hypochlorite (NaOCl) and *tert*-butyl hydroperoxide (t-BuO$_2$H). These types of oxidants, which are called single oxygen donors, are economically attractive and usually environmentally acceptable. From the industrial point of view, the most important properties of single oxygen donors are the type of by-products that should be easily disposable or recyclable. Considering the costs of the production, the molecular weight per active oxygen should be as low as possible. Typically, the most attractive commercial single oxygen donors are hydrogen peroxide, sodium hypochlorite and *tert*-butyl hydroperoxide.

Activation of Alkyl hydroperoxide and Hydrogen Peroxide

Peroxides, such as hydrogen peroxide and alkyl hydroperoxides, are among the most important classes of single-oxygen donors used in organic synthesis. The reaction catalyzed by metal ions using peroxides as oxidants can be divided into two groups. The first group involves homolytic, one-electron processes in which free radicals appear as intermediates. Fenton chemistry is a well-known example of this type of reaction.[34] The mild oxidizing activity of hydrogen peroxide is considerably enhanced in the presence of a ferrous salt. In aqueous media, hydrogen peroxide interacts with Fe(II) complex producing •OH radicals. The subsequent reactivity of •OH radicals with organic substrates via H-atom abstraction yields alkyl radicals, which propagate chain reactions

The yields of oxidized substrates are often low for the oxidation reactions using Fenton's reagents. This is because the non-productive decomposition of H_2O_2 takes place during time as a competitive reaction,

The metal catalyzed homolytic decomposition of alkyl hydroperoxides formed as the results of reactions from Equation 1 16 to 1 20 is the most common further transformations taking place in the autoxidation of hydrocarbons Two principal reactions of alkyl hydroperoxides with metal complexes may be considered, depending on the reduction potential of the metal When metal complex has strong reducing properties, reduction takes place

$$RO_2H + M^{(n-1)+} \longrightarrow RO\bullet + M^{n+} + HO \qquad (1\ 16)$$

Whereas with metal complex with oxidizing power, oxidation occurs

$$RO_2H + M^{n+} \longrightarrow RO_2\bullet + M^{(n-1)+} + H^+ \qquad (1\ 17)$$

A series of further radical reactions are followed

$$2\,RO_2\bullet \longrightarrow 2\,RO\bullet + O_2 \qquad (1\ 18)$$

$$RO\bullet + RO_2H \longrightarrow RO_2\bullet + ROH \qquad (1\ 19)$$

$$RO\bullet + R'H \longrightarrow R\bullet + ROH \qquad (1\ 20)$$

In this case, transition metal complex acts as an "initiator' for the reaction rather than a "catalyst" Complexes of such metals as cobalt and manganese have two oxidation states of comparable stability So, both reaction (1 16) and (1-17) proceed and catalytic decomposition of alkyl hydroperoxides takes place (Equation 1 21)

$$2\,\mathrm{ROOH} \xrightarrow{\text{Co, Mn salts}} 2\,\mathrm{ROH} + \mathrm{O_2} \qquad (1.21)$$

These radical reactions are generally characterized by low selectivity and therefore are limited in their applicability However, considerable efforts have been devoted to finding means by which hydroperoxides can be stabilized for periods long enough to undergo a selective reaction to form more stable oxidation products

Instead of metal-catalyzed homolytic decomposition of alkyl hydroperoxides hydroperoxide can coordinate to a metal complex in such a way that its terminal peroxy oxygen is rendered more electrophilic and hence, more susceptible to reactions with π-electron systems of olefins Oxygen transfer in a two-electron reaction of heterolytic cleavage of the O-O bond follows (Equation 1.22) Such reactions are usually much more selective.

$$\mathrm{S} + \mathrm{RO_2H} \longrightarrow \mathrm{SO} + \mathrm{ROH} \qquad (1.22)$$

Since the epoxidation of olefins is a very important industrial application of homogeneous oxidation and activation of saturated hydrocarbons the most prospective, these two type of reactions will be discussed in detail

Catalytic Epoxidation of Olefins

Epoxidation is a very important reaction with significant synthetic applications.[5] Organic peracids are generally used to carry out epoxidation reactions Safety and environmental concerns have led to searching alternative epoxidizing reagents to replace organic peracids. Alkyl hydroperoxide and hydrogen peroxide are the best candidates for the catalytic epoxidation reactions On the other hand, transition metal-catalyzed oxidation of alkenes with molecular oxygen generally goes through radical reaction pathway, which leads primarily to allylic oxidation products via autoxidation rather than epoxides

In most case, alkyl hydroperoxide and hydrogen peroxide are not strong epoxidizing reagents to perform epoxidation efficiently Several methods to activate alkyl hydroperoxide are devised One way is generating peracid in situ In the case of using H_2O_2, the following equilibrium can be reached (Equation 1 23).

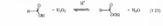

$$RCOOH + H_2O_2 \underset{}{\overset{H^+}{\rightleftharpoons}} RCOOOH + H_2O \qquad (1\ 23)$$

The peracid further reacts with olefin in the solution to form epoxide (Figure 1 7)

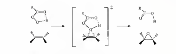

Figure 1 7: Epoxidation of olefins by peracid [16]

There are two major drawbacks in this method The amount of H_2O in the system will increase during the reaction, which leads to shifts of the equilibrium (Equation 1 23) away from the formation of peracid Thus the epoxidation reaction will slow down in the presence of significant amount of H_2O A separation procedure is needed to continuously remove H_2O out of the reaction system. Also, the side reaction of acid-catalyzed epoxide ring opening will decrease the yield of formation of epoxide (Equation 1.24) [17]

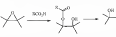

(1.24)

Transition metal complexes can also activate alkyl hydroperoxides and hydrogen peroxide for the epoxidation of olefins. The suggested mechanism involves the formation of a hydroperoxide complex (Figure 1.8).[18] The nature of transition metal catalyzed epoxidation reaction consists of the nucleophilic attack of the olefin. The catalyst is functioned as a Lewis acid to withdraw electrons from the peroxidic oxygen, rendering them more susceptible to this nucleophilic attack.

Theoretically, good epoxidation catalysts have high Lewis acidity on the metal centers. These transition metals are often in their highest oxidation state. The order of Lewis acidity of transition metal oxides is $CrO_3 > MoO_3 > WO_3 > TiO_2 > V_2O_5 > UO_3$ [19] That is why common epoxidation catalysts are Mo(VI), W(VI) and Ti(IV) complexes. ARCO process utilizes a homogeneous molybdenum catalyst in conjunction with an alkyl hydroperoxide for the production of propene oxide through epoxidation of propene.[20]

Although Cr(VI) is a strong Lewis acid, it is a poor epoxidation catalyst. The oxidation ability of Cr(VI) accelerates the hydrogen abstraction reaction by formation of allylic oxidation products. For the same reason, first row transition metals in their highest oxidation states are usually not good epoxidation catalysts because these metals either decompose the peroxides or do allylic oxidation.

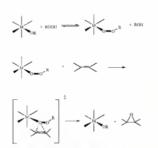

Figure 1.8 General mechanism of transition metal catalyzed epoxidation reaction.

Selective Catalytic Oxidation of Saturated Hydrocarbons

The activation of C-H bonds in saturated hydrocarbons is one of the most difficult challenges facing chemists. The primary deterrent in the activation of alkanes is the chemical inertness of these molecules. The second obstacle is that it is very hard to control the alkane oxidation reaction. This is because the useful oxidation products, such as alcohol, aldehyde and ketone, are much easier to oxidize than the corresponding alkane Once the alkane is activated, it is very easy to get over oxidized products, which generate CO_2 and CO

The inertness of alkanes may be attributed to their high C H bond energies The value of the C-H bond dissociation energy for methane is 104 kcal mol $^{-1}$ But, ethylene, acetylene, and benzene, which have stronger C H bonds (106, 120, 109 kcal mol $^{-1}$, respectively) than methane, are very active towards oxidation reactions. So the lack of either π- or n-electrons in saturated hydrocarbon molecules may attribute to their inertness. Conversely, the π- or n-electrons of unsaturated hydrocarbons allow most of their reactions to proceed by addition, followed in some case by elimination.

Based on the mechanism of catalytic oxidation of saturated hydrocarbon, Shilov[21] classified C-H bond splitting reactions into three groups

(1) "True" Activation It corresponds to the formation of an organometallic derivative containing an M-C σ-bond as an intermediate or as final product. The reason they call this type of activation " true" is that in this case there is a close contact between a metal ion and a C-H bond. The cleavage of the C-H bond by direct participation of a transition metal ion proceeds via oxidative addition mechanism (Equation 1.25), or an electrophilic substitution mechanism (Equation 1 26)

$$RH + M^{n+} \longrightarrow R-M^{(n+2)+}-H \qquad (1\ 25)$$

$$RH + M^{n+} \longrightarrow R-M^{n+} + H^{+} \qquad (1\ 26)$$

(2) No direct contact between the metal and the C-H bond. The role of transition metal catalyst in the reaction is obstracting an electron or a hydrogen atom from hydrocarbon. No M-C σ-bond is formed in this group. The metal-oxo complex such as CrO_4^{2-}, MnO_4^- or an oxoferryl species serves as an oxidant (Equation 1.27)

$$RH + O{=}M^{n+} \longrightarrow R\bullet + HO\text{-}M^{(n-1)+} \longrightarrow ROH + M^{(n-2)+} \qquad (1.27)$$

(3) A metal complex promotes the formation of a reactive species, which then attacks the C-H bond. Other reactants (e.g., O_2 or H_2O_2) can be activated by metal catalyst to form a reactive species, which then attacks the hydrocarbon molecule. The reactive species is usually a radical, such as a hydroxyl radical. The oxidation of alkanes by Fenton's reagent (Fe^{2+}/H_2O_2) is a typical example of such a process.

Conclusions

The essence of catalysis can be described briefly as the art of manipulating chemical molecules. Homogeneous catalytic oxidation is a productive field which needs to be further explored. The current explanations to the mechanism of the oxidation reactions are far from satisfied. The general way for developing a new catalyst is still by a "random screening" approach. Even with the new combinatorial method, it simply speeds up the screening process. Some current industrial oxidation processes were developed in 1930's and 1940's. Despite some big disadvantages of using these processes, for example they may cause serious environmental problem, chemists are still struggling to find better catalysts to replace the currently used catalysts, which have been used for 50 years. So the catalytic homogeneous oxidation reactions will continue to be of major interest for chemists and the big driving force from petroleum chemistry and fine chemical industry will keep this area intensely investigated in the new millennium.

CHAPTER 2
SINGLE STEP SYNTHESIS OF SOLID ADIPIC ACID BY CATALYTIC OXIDATION OF CYCLOHEXANE IN AIR

Introduction

Adipic acid (hexanedioic acid $HOOC(CH_2)_4COOH$) is a linear six carbon molecule containing two carboxylic groups. The major use of adipic acid in industry is for the manufacture of polyamides, which are mostly nylon-6,6 and some paper additives. The reaction for making nylon-6,6 involves the condensation and polymerization of adipic acid with 1,6-diaminohexane (Equation 2.1)[22]

$$nH_2N(CH_2)_6NH_2 + nHO_2C(CH_2)_4CO_2H \longrightarrow [\ O_2C(CH_2)_4CO_2\ NH_2(CH_2)_6NH_3^+\ ]_n$$

nylon 6,6 salt

$$\xrightarrow{> 265\ ^{\circ}C} HO[CO(CH_2)_4CONH(CH_2)_6NH]_nH + (2n - 1)\,H_2O \qquad (2\ 1)$$

nylon- 6 6

Nylon-6 6 can further condense with epoxides to form high-efficiency, cationic wet strength resins which are typically used for making ink cartons fineboard, toweling and tissues (Equation 2.2).[23]

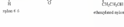

(2 2)

Polyesters are the second most important class of adipic acid derivatives next to polyamides. Polyesters are synthesized by the condensation reaction between adipic acid and alcohols such as 1,6-hexanediol (Equation 2.3). The esters are marketed as plasticizers for PVC, natural and synthetic adhesives, polystyrene and cellulose derivatives and synthetic ester lubricants.[24]

$$\underset{\text{Excess}}{\text{HO-R-OH} + n\ \text{HOOC(CH}_2)_4\text{COOH}} \xrightarrow{140\text{ - }220\ ^\circ\text{C}}$$

$$\text{HO-R-O-[CO(CH}_2)_4\text{COO-R-O]}_n\text{-H} + \text{H}_2\text{O} \qquad (2.3)$$

Adipic acid also can be used to synthesize some chemical products. For example, 1,6-diaminohexane can be produced from adipic acid by converting it into the corresponding diamide, which is then dehydrated to adiponitrile. Hydrogenation of adiponitrile gives 1,6-diaminohexane (Equation 2.4).[25]

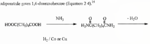

$$\text{HOOC(CH}_2)_4\text{COOH} \xrightarrow{\text{NH}_3} \text{H}_2\text{N}\overset{\text{O}}{\overset{\|}{\text{C}}}(\text{CH}_2)_4\overset{\text{O}}{\overset{\|}{\text{C}}}\text{NH}_2 \xrightarrow{-\text{H}_2\text{O}}$$

$$\underset{\text{Adiponitrile}}{\text{NC(CH}_2)_4\text{CN}} \xrightarrow[125^\circ\text{C}, 600\text{ atm}]{\text{H}_2\text{ / Co or Cu}} \text{H}_2\text{N(CH}_2)_6\text{NH}_2 \qquad (2.4)$$

Adipic acid with high purity can be used as a food additive, which is approved by the Food and Drug Administration as "generally recognized as safe". Generally, Adipic acid is used in desserts, fruit-flavored beverages, jams, jellies, precooked food and canned vegetables as a food acidulant.[24]

The production of adipic acid in the United States is about 7.44 × 10^5 tons each year, which accounts for 30 % of adipic acid production worldwide.[26] The currently favored industrial process for making adipic acid uses nitric acid as oxidant. Nitrous oxide (N_2O) is generated as a by product (Equation 2.5).[27]

$$C_6H_{11}OH / C_6H_{10}O + HNO_3 \rightarrow \text{Adipic Acid} + aN_2 + bNO + dN_2O \quad (2.5)$$

The reaction stoichiometry is about 1 mole of N_2O per mole of adipic acid. Nitrous oxide is unambiguously implicated in environmental problems such as catalytic ozone destruction, acid rain and smog. Estimates show that the amount of nitrous oxide generated by the current adipic acid process may account for about 10 percent of the overall increase observed for atmospheric N_2O.[27]

Several attempts have been made to develop a one-step air or peroxide oxidation of cyclohexane for the preparation of adipic acid in order to solve the environmental problems generated by the current industrial adipic acid process. These efforts mostly used a Co (III) catalyst in acetic acid medium under high oxygen pressure (20-30 atm).[28]

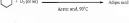

(2.6)

This one-step air oxidation process (Equation 2.6) can reach 80% conversion and 70% selectivity. However, the formation of by-products in the one-step oxidation process necessitated the costly product purification steps in the plant design, which makes the two-step process still preferred in industry.

A mechanistic investigation showed that the reaction is not a classical free-radical oxidation in which peroxy and alkoxy radicals serve as a hydrogen abstracting substance but a catalytic reaction by Co (III) and Co (II). The possible mechanism is shown in Figure 2.1.[28d, 29]

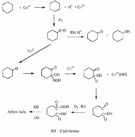

Figure 2.1: Possible mechanism of cobalt catalyzed air oxidation cyclohexane to adipic acid.

The cobalt-catalyzed, air oxidation of cyclohexane shows that glutaric acid ($HOOCC_3H_6COOH$) and succinic acid ($HOOCC_2H_4COOH$) constitute a significant percentage of the identifiable products approximately 20 mole% at 90°C and 50 mole% at 150°C [30] Those results suggest that the instability of adipic acid contributes to the poor overall selectivity Results from another experiment showed that at high concentration of cobalt catalyst (> 0 15 M), adipic acid is indeed converted to lower acids in the presence of hydrocarbon. The ratio of adipic acid to glutaric acid to succinic acid is about 4 7 1 1 [31] The coordination of cobalt salt to adipic acid, which promotes the degradation of adipic acid, was proposed The decarboxylation of carboxylic acid during the autoxidation of cyclohexane is shown as below (Equation 2 7)

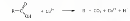

$$R{-}C(=O)OH + Co^{3+} \longrightarrow R + CO_2 + Co^{2+} + H^+ \qquad (2\ 7)$$

The formation of by-products such as glutaric acid and succinic acid is more complicated than expected Other results gave opposite conclusion Some results revealed that at low catalyst concentration (~0 05 M ($Co(OAc)_2\ 4H_2O$, OAc = acetate) the major route to glutaric and succinic acid is not via decarboxylation of adipic and glutaric acids. Only <3% of the adipic acid decomposed at 90°C and at 150°C > 12% of the adipic acid decarboxylated.[32]

Most literature reported one-step oxidation of cyclohexane to adipic acid used soluble cobalt and manganese salts such as $Co(OAc)_2\ 4H_2O$ as catalyst One paper reported ferric chloride ($FeCl_3$) -catalyzed aerobic oxygenation of 2-halocyclohexanones (**1**) in methanol to yield adipic acid dimethyl esters (**2**) (Equation 2.8) [33] Using non halogenate ketone, 2-methylcyclohexone (3), at same reaction conditions gives exclusively methyl 6-oxoheptanoate (4) (Equation 2.9). On the other hand, ferrous salt, FeCl$_2$, showed no catalytic activity in aerobic oxidation of (1) to (2), but catalyzed the dehydrohalogenation producing (5) (Equation 2.10). The amount of FeCl$_3$ used greatly affects the reaction pathways. The formation of the dehydrohalogenation product of (5) competed the oxygenation product of (2), when < 10 mole % of FeCl$_3$ was used. Using > 30 mole % of FeCl$_3$ generated more adipic acid dimethyl esters (2).

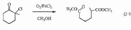

(2.8)

(1) (2)

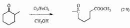

(2.9)

(3) (4)

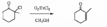

(2.10)

(1) (5)

Draths reported an environmentally compatible bio-synthesis of adipic acid from D-glucose using microbial catalyst. D-glucose was first converted into *cis,cis*-muconic acid (HOOCCH=CH-CH=CHCOOH). Subsequent catalytic hydrogenation of *cis,cis*-muconic acid affords adipic acid (Equation 2.11). The starting material D-glucose is nontoxic and can be obtained from biological source such as plant starch and cellulose. This is a very promising process for making adipic acid while the optimization and scale up of the reaction are problems, which are not easy to solve.[34]

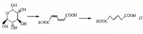

(2.11)

D-glucose　　*cis,cis*-muconic acid　　adipic acid

Sato recently reported a route in which cyclohexene is oxidized directly to adipic acid with 30% H_2O_2.[35] The reaction is catalyzed by tungsten catalyst combined with a phase-transfer agent. The reaction pathway is shown in Figure 2.2. There is no air pollution and only water is by-product. High yield of adipic acid (90%) can be achieved. However, the cost of the H_2O_2 as oxidant is much higher than that of air for the use in industrial processes. Therefore, this process will be attractive only if the cost of H_2O_2 is considerably reduced or if the regulations regarding nitrous oxide become more stringent.

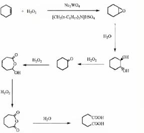

Figure 2.2: The reaction pathway for the direct oxidation of cyclohexane to adipic acid with aqueous H_2O_2

Catalytic oxidation of saturated hydrocarbons has been extensively studied in our laboratory and several related papers were published recently.[36] Our research demonstrates that transition metal complexes such as Fe-dpphen (dpphen = 4,7 diphenyl-1,10-phenanthroline) and Ru-dmpphen (dmpphen = 2,9-dimethyl-4,7-diphenyl-1,10-phenanthroline) are able to catalyzes oxidation of cyclohexane to solid adipic acid under mild conditions using air as oxidant.

Experimental

Reagents and Equipment

Unless otherwise stated, all reagents were obtained from commercial sources and used without further purification. All solvents were distilled and stored over 4Å molecular sieves before use. Gas chromatographic analyses on volatile products and reactants were carried out by using a Hewlett Packard model 5890 gas chromatograph equipped with Hewlett Packard 50+ column (crosslinked 50% phenyl methyl – 30 m × 0.53 mm × 1.0 μm film thickness). Helium was used as the carrier gas for the gas chromatograph with a flame ionization detector, and a Hewlett Packard 3396 Series II integrator. Substrates and products were identified via comparisons with known standards. Calibration curves were used to relate peak areas to the number of moles of products and reactants. Infrared spectroscopy was performed on a Nicolet 5PC equipped with 1MW He-Ne laser and Nicolet PCIR software (Version 3.2). ^1H and ^{13}C NMR spectra were obtained on a Gemini 300 spectrometer. Elemental analysis data were performed by spectral services at the University of Florida.

Preparation of Fe(dpphen)$_3$(CF$_3$SO$_3$)$_2$

Ten mL of 1 M AgCF$_3$SO$_3$ aqueous solution was added to 10 mL of 0.5 M FeCl$_2$ aqueous solution. White precipitate (AgCl) was formed immediately. Further stirring the solution for approximately 3-4 hours, the white precipitate was filtered off and a clear Fe(CF$_3$SO$_3$)$_2$ solution was generated. After adding 30 mL of 0.5 M dpphen ethanol solution to Fe(CF$_3$SO$_3$)$_2$ solution, a deep red solution was resulted. Further stirring the solution for about 3 hours to reduce the volume of solvent to about 10mL, a large crop of red product was formed. The precipitate was then washed three times with small quantities of above solvent, and dried in a vacuum oven at 60 °C for at least 12 hours. A red powder was obtained as the final product (yield 85%). Element analyses: Anal. Calcd. for $Fe_1C_{74}H_{48}N_6O_6F_6S_2$ (%): C, 65.78, H, 3.58, N, 6.22. Found (%): C, 65.66, H, 3.53, N, 6.13. Electron spray ionization mass spectroscopy (ESI-MS) for $Fe(dpphen)_3(CF_3SO_3)_2$: MW = 1053 ($Fe(dpphen)_3^{2+}$), MW = 869 ($Fe(dpphen)_2(CF_3SO_3)^+$), MW = 720 ($Fe(dpphen)_2^{2+}$), MW = 333 ($Hdpphen^+$)

Preparation of $Fe(dpphen)_3(ClO_4)_2\bullet 0.5H_2O$

Three mmole of dpphen ligand was dissolved in 200 mL of C_2H_5OH. 2 mmole of $Fe(ClO_4)_2$ was added to the above solution. A deep red solution was resulted. Further stirring the solution for about 2 hours, a large crop of red product was formed. The precipitate was then washed three times with small quantities of above solvent, and dried in a vacuum oven at 65°C for 6 hours. A red powder was obtained as the final product (yield 87%). Element analyses: Anal. Calcd. for $Fe_2C_{144}H_{98}N_{12}O_{17}Cl_4$ (%): C, 68.58, H, 3.92, N, 6.66. Found (%): C, 68.64, H, 3.73, N, 6.68.

General Procedure for Oxidation of Cyclohexane with Air

Oxidation reactions were carried out in a batch reactor as previously described.[37] A typical reaction consisted of the following in solution: cyclohexane (5 mL), organic co-solvent (10 mL), catalyst (8.89×10^{-6} mol), and chlorobenzene (0.2 mL) which served as an internal standard. Each reaction was pressurized with air to 45 psi, and placed in an oil bath with a constant temperature. At the conclusion of the reaction period, the reactor was taken out off the oil bath and allowed to cool. The pressure was released and the reactor was disassembled. Reactant consumption and reaction products in the liquid phase were monitored and quantified by GC. The moles of each of the reactants and the known products were determined by using calibration curves for each compound. The solid reaction products were separated by filtration, washed with small amount of CH_3CN and dried in a vacuum oven at 90 °C for at least 12 hours. Element analyses: Anal. Calcd. for adipic acid $C_6H_{10}O_4$ (%): C, 49.3, H, 6.9, N, 0. Found (%): C, 48.8, H, 6.7, N, 0.06. Electron spray ionization mass spectroscopy (ESI-MS) for adipic acid ($C_6H_{10}O_4$) MW = 147.1 ($C_6H_{10}O_4H^+$)

The combination of molecular oxygen with organic compounds and solvents at elevated temperatures and pressures is a potential explosive. Extreme caution should be taken during the charging and disassembly of the experimental apparatus, particularly around the equipement that generates sparks. The use of safety shield and allowing the reaction to cool prior to disassembly is highly recommended.

Determination of the Crystal Structure of $Fe(dpphen)_3(CF_3SO_3)_2 \cdot 5(CH_3C(OH)CH_3)$

Data were collected at 173 K on a Siemens SMART PLATFORM equipped with A CCD area detector and a graphite monochromator utilizing MoK_α radiation (λ = 0.71073 Å). Cell parameters were refined using 8192 reflections. A hemisphere of data (1381 frames) was collected by using the ω-scan method (0.3° frame width). The first 50 frames were re-measured at the end of data collection to monitor instrument and crystal stability (maximum correction on I was < 1 %). Absorption corrections by integration were applied based on measured indexed crystal faces.

The structure was solved by the Direct Methods in *SHELXTL5* and refined using full matrix least squares. The non H atoms were treated anisotropically, whereas the hydrogen atoms were calculated in ideal positions and were riding on their respective carbon atoms. A total of 957 parameters were refined in the final cycle of refinement using 9182 reflections with $I > 2\sigma(I)$ to yield R_1 and wR_2 of 6 25% and 15 58%, respectively Refinement was done by using F^2 [36]

Results and Discussion

Synthesis and Structure Determination of $Fe(dpphen)_3(CF_3SO_3)_2$ (6)

The catalyst 6 was prepared by addition of dpphen in C_2H_5OH to an aqueous solution of $Fe(CF_3SO_3)_2$ Recrystalization in 2-propanol gave the suitable single crystal for the structure determination The crystal structure and crystal data obtained are provided in Figure 2 3 and table 2 1-2.3

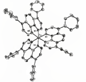

Figure 2.3 Structure of catalyst **1** ORTEP view of the cation of $Fe(dpphen)_3(CF_3SO_3)_2$

Table 2.1. Crystal data and structure refinement for Fe(dpphen)$_3$(CF$_3$SO$_3$)$_2$

Identification code	Fedpphen	
Empirical formula	C89 H83 F6 Fe N6 O11 S2	
Formula weight	1646.58	
Temperature	173(2) K	
Wavelength	0.71073 Å	
Crystal system	Orthorhombic	
Space group	Pna2(1)	
Unit cell dimensions	a = 21.281(1) Å	α= 90°
	b = 12.1468(5) Å	β= 90°
	c = 31.444(1) Å	γ = 90°
Volume	8128.1(6) Å^3	
Z	4	
Density (calculated)	1.346 Mg/m^3	
Absorption coefficient	0.316 mm^{-1}	
F(000)	3436	
Crystal size	0.08 x 0.11 x 0.46 mm^3	
Theta range for data collection	1.80 to 25.00°	
Index ranges	-22<h<25, -14<k<14, -37<l<35	
Reflections collected	55924	
Independent reflections	13067 [R(int) = 0.0570]	
Completeness to theta = 25.00°	100.0 %	
Absorption correction	Integration	
Max. and min. transmission	0.9780 and 0.9392	
Refinement method	Full-matrix least-squares on F^2	
Data / restraints / parameters	13067 / 1 / 957	
Goodness-of-fit on F^2	1.039	
Final R indices [I>2sigma(I)]	R1 = 0.0625, wR2 = 0.1558 [9182]	
R indices (all data)	R1 = 0.0977, wR2 = 0.1760	
Absolute structure parameter	0.10(3)	
Extinction coefficient	0.00028(14)	
Largest diff. peak and hole	0.837 and -0.462 e.Å^{-3}	

Table 2 2. Selected bond lengths [Å] for Fe(dpphen)$_3$(CF$_3$SO$_3$)$_2$

Fe-N3	1.954(5)
Fe-N2	1.960(5)
Fe-N5	1.962(5)
Fe-N1	1.972(5)
Fe-N4	1.973(5)
Fe-N6	1.978(6)
N1-C1	1.343(7)
N1-C5	1.379(8)
N2-C10	1.352(7)
N2-C6	1.354(8)
C1-C2	1.404(8)
C2-C3	1.376(8)
C3-C4	1.445(8)
C3-C13	1.475(9)
S1-O1	1.387(6)
S1-O3	1.413(6)
S1-O2	1.466(8)
S1-C73	1.807(11)
C73-F3	1.253(12)
C73-F2	1.308(12)
C73-F1	1.318(11)

Table 2.3 Selected bond angles [°] for $Fe(dpphen)_3(CF_3SO_3)_2$

N3-Fe-N2	89.4(2)
N2-Fe-N5	94.2(2)
N3-Fe-N1	94.8(2)
N2-Fe-N1	82.0(2)
N5-Fe-N1	89.69(13)
N2-Fe-N4	95.0(2)
N1-Fe-N4	176.1(2)
N2-Fe-N6	174.17(15)
N1-Fe-N6	93.1(2)
C1-N1-C5	117.0(5)
C1-N1-Fe	129.2(4)
C5-N1-Fe	113.8(4)
C10-N2-C6	116.0(5)
C10-N2-Fe	129.3(4)
C6-N2-Fe	114.6(4)
N1-C1-C2	122.3(6)
C3-C2-C1	121.8(6)
C2-C3-C4	116.8(6)
C2-C3-C13	120.8(6)
C4-C3-C13	122.3(6)
O1-S1-O3	114.7(5)
O1-S1-O2	115.5(6)
O3-S1-O2	114.0(5)
O1-S1-C73	103.7(5)
O3-S1-C73	103.7(5)
O2-S1-C73	103.0(5)
F3-C73-F2	109.1(9)
F3-C73-F1	105.7(10)
F2-C73-F1	105.7(10)
F3-C73-S1	114.4(8)
F2-C73-S1	110.2(8)
F1-C73-S1	111.2(8)

Symmetry transformations used to generate equivalent atoms

The X-ray crystal structure of Fe(dpphen)$_3$(CF$_3$SO$_3$)$_2$ reveals that the three bidentate dpphen ligands coordinate with the iron center and the two triflates (CF$_3$SO$_3^-$) serve as non-coordinating counter anions The six Fe-N bond lengths are almost equal ranging from 1 954 to 1 978Å, which generates a slightly distorted octahedral coordination geometry The substituted phenyl rings in each dpphen ligands are not co-planar with the central part of the ligand with the distortion angles around 50 °

Oxidation of Cyclohexane to Adipic Acid

Under our reaction conditions (140 °C, 90psi of air and 5 9 × 10^{-4} M of catalyst), cyclohexane is oxidized to a 1 7 1 6 0 mixture of adipic acid, cyclohexanone and cyclohexanol in 5 hours (21 turnovers to acid, 149 turnovers to ketone and 126 turnovers to alcohol)

Table 2 4. Catalytic Oxidation of Cyclohexane [a]

Temp (°C)	Adipic Acid (×10^{-4} mol)	Ketone (×10^{-4} mol)	Alcohol (×10^{-4} mol)
140	3 7	26 3	22 1
130	2 7	18 3	13 8
120	1 6	10.6	9 3
110	0 01	4 4	4 7

[a] The oxidation reactions were carried out in a batch reactor using a 300 ml titanium autoclave (Parr Instrument) The reactions consisted of the following catalyst (1 76 × 10^{-5} mol), o-dichlorobenzene (20 mL), cyclohexane (10 mL) The pressure apparatus was placed into a constant-temperature mantle and pressurized with 90psi of air Reactions were run for 5 hours

The catalytic oxidation is very sensitive to the reaction temperature (Table 2 4) At 100 °C with the other reaction conditions identical only a trace amount of cyclohexanone was observed as the product. Further increasing the temperature to above 140 °C, a black precipitation was found, which suggests the increasing formation of byproducts and decomposition of the catalyst.

The lack of a significant induction period is demonstrated through the variation of the reaction time experiments. Significant amounts of adipic acid, cyclohexanone, and cyclohexanol were detected for a 1 hour reaction at 120 °C. Higher amounts of adipic acid, cyclohexanone, and cyclohexanol were observed with longer reaction time (Figure 2.4).

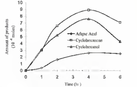

Figure 2.4: Time dependence of the cyclohexane oxidation.

The catalyst generated *in situ* has lower reactivity than the isolated solid catalyst **6**. The insolubility of the iron (II) salt ($Fe^{II}(CF_3SO_3)_2$) in the reaction system causes the difficult for the formation of active compound, which may account for the lower reactivity of *in situ* generated catalyst. Changing the counter-anion of the catalyst **6** from triflate ($CF_3SO_3^-$) to perchlorate (ClO_4^-) does not effect the catalytic reactivity within the experiment error (Table 2.5).

Table 2.5 Influence of the counter-anion of catalyst on the catalytic oxidation of cyclohexane [a]

Catalyst	Acid ($\times10^{-4}$ mol)	Ketone ($\times10^{-4}$ mol)	Alcohol ($\times10^{-4}$ mol)
$Fe(dpphen)_3(CF_3SO_3)_2$	2.5	7.1	4.3
$Fe(dpphen)_3(CF_3SO_3)_2$[b]	1.5	8.3	4.7
$Fe(dpphen)_3(ClO_4)_2$	2.7	8.4	3.3

[a] The oxidation reactions were carried out in a glass bottle batch reactor. The reactions consisted of the following: 1.76×10^{-5} mol iron (II) catalyst, *o*-dichlorobenzene (10 mL), cyclohexane (5 mL). The pressure apparatus was placed into a constant-temperature mantle and pressurized with 3 atm of air at 120°C. Reactions were run for 6 hours. Experiment error were estimated by running reaction four times using $Fe(dpphen)_3(CF_3SO_3)_2$ as catalyst. The results were adipic acid, ±15%, cyclohexanone ± 20%, cyclohexanol ±25%.

[b] catalyst generated *in situ*.

Variation of the ligand to metal ratio experiments showed that highest reactivity occurred at 2:1 and 3:1 ligand to metal ratio. Less adipic acid was recovered when ligand to metal ratio equals to 6:1 (Table 2.6).

The current industrial adipic acid process generate numerous byproducts, such as formic acid, acetic acid, butyric acid, valeric acid, *etc*.[39] There are no detectable amounts of formic acid, acetic acid, butyric acid and valeric acid generated in our reaction system. Several unidentified byproducts, excluding cyclohexanone and cyclohexanol, were found in the liquid phase by comparing the GC analysis results before the reaction to those after the reaction (Figure 2.5). By comparison the peak areas of byproducts with those of cyclohexanone and cyclohexanol, the formation of by-products in liquid phase is less than 5%. We also detected the formation of small amounts of CO, CO_2 and H_2O in the gas phase by using GC, but the amounts have not been quantified. The isolated adipic acid was analyzed by using elemental analysis, mass spectroscopy and NMR (Figure 2.6). All results showed that the isolated adipic acid is very pure (>95%).

Table 2.6 Influence on catalytic oxidation of cyclohexane by variation of ligand to metal ratio

Metal : Ligand	Adipic Acid ($\times 10^{-4}$ mol)	Ketone ($\times 10^{-4}$ mol)	Alcohol ($\times 10^{-4}$ mol)
1 : 1	0.4	3.0	3.3
1 : 2	1.4	8.8	5.9
1 : 3	1.5	8.3	4.7
1 : 6	Trace	7.5	3.5

[a] The oxidation reactions were carried out in a glass bottle batch reactor. The reactions consisted of the following: $Fe(CF_3SO_3)_2$ (1.76×10^{-5} mol), certain amounts of dyphen, o-dichlorobenzene (10 mL), cyclohexane (5 mL). The pressure apparatus was placed into a constant temperature mantle and pressurized with 45psi of air. Reactions were run for 6 hours.

Figure 2.5 GC analysis results for liquid sample after reaction (left) and before reaction (right).

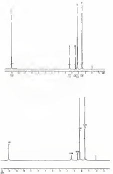

Figure 2.6 ^{1}H NMR spectrum for isolated solid product (top) and adipic acid (bottom)

Various additives have been extensively studied for cyclohexane oxidation to provide information on the mechanism of the reaction (Table 2.7). The addition of a free-radical inhibitor, benzoquinone, to the reaction quenched of the oxidation reaction.

Table 2.7. Catalytic oxidation of cyclohexane with different additives [a]

Additive	Amounts ($\times 10^{-4}$ mol)	Adipic Acid ($\times 10^{-4}$ mol)	Cyclohexanone ($\times 10^{-4}$ mol)	Cyclohexanol ($\times 10^{-4}$ mol)
Water	56	1.2	8.6	4.4
Pyridine	2.5	0.51	6.2	3.2
Acetic Acid	3.3	1.3	8.2	3.8
AIBN	0.1	1.6	7.4	7.3
AIBN (no cat.)	0.1	0	trace	0
Benzoquinone	89	0	0	0
CHP	8.5	2.4	6.9	6.4
CHP (no cat.)	8.5	0	2.5	3.8
—	0	1.3	7.4	5.9
No cat./add	8	0	trace	trace

[a] The oxidation reactions were carried out in a batch reactor using a 250 mL glass bottle reactor. The reactions consisted of the following: catalyst (8.8×10^{-6} mol), *o*-dichlorobenzene (10 mL), cyclohexane (5 mL). The pressure apparatus was placed into a constant temperature oil bath at 120 °C and pressurized with 45psi of air. Reactions were run for 3 hours.

Adding AIBN (AIBN = 2,2'-azobisisobutyronitrile), a free radical initiator, to the *o*-dichlorobenzene solution containing the iron catalyst had no effect on the reaction, while AIBN alone did not initiate the reaction. These experiments indicate a catalyzed free radical chain mechanism. Adding a small amount of H_2O had no effect on the reactivity of the catalyst and the product distribution. The catalyst **6** was tolerant for at least small amounts of acid but suffered with small amounts of base.

Cyclohexylhydroperoxide (CHP) is believed to be an intermediate formed in cyclohexane oxidation. In the current industrial process, cyclohexane is first autoxidized to CHP, which is subsequently decomposed to cyclohexanone and cyclohexanol in the presence of cobalt catalyst. Adding CHP to our reaction system significantly enhanced the yield of adipic acid, while the amount of cyclohexanone and cyclohexanol produced were unchanged within experimental error. When CHP was added to the reaction system without iron catalyst, only cyclohexanone and cyclohexanol were formed, which can be attributed to the decomposition products of CHP.

Because dioxygen is a limiting reagent for the oxidation of cyclohexane under our reaction conditions, large amounts of cyclohexanone and cyclohexanol are generated. Recharging air to the reactor without separation showed the amount of cyclohexanone reaches steady state concentration and the amount of cyclohexanol decreases while the production of adipic acid keeps increases (Figure 2.6). Those results clearly indicate the conversion of cyclohexanone and cyclohexanol to adipic acid.

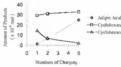

Figure 2.6: Air recharging reaction of oxidation of cyclohexane [a]

[a] The oxidation reactions were carried out in a batch reactor using a 300 ml titanium autoclave (Parr Instrument). The reactions consisted of the following: catalyst (1.76 × 10^{-5} mol), *o*-dichlorobenzene (20 mL), cyclohexane (10 mL). The apparatus was pressurized with 100psi of air. Reaction temperature was 120 °C and reactions were run for 11-12 hours for each cycle. At the conclusion of each reaction period, the reactor was taken out off the oil bath and allowed to cool. The pressure was released and recharged with 100psi of air.

Other Experiments

Iron (III) tetra-(pentafluorophenyl) porphyrin chloride has been reported as the most active catalyst for hydrocarbon autoxidation reactions.[40] Under our reaction conditions, using the reported Fe-porphyrin catalyst generated large amounts of cyclohexanone and cyclohexanol but no adipic acid was found. Several transition metal compounds were tested for the oxidation of cyclohexane.

Ru(dmpphen)$_2$Cl$_2$ showed good catalytic activity towards the formation of adipic acid, cyclohexanone and cyclohexanol. However, unlike Fe(dpphen)$_2$(CF$_3$SO$_3$)$_2$, a much longer reaction period (43 hours) was required and a significant induction period

Table 2.8. Catalytic oxidation of cyclohexane with different catalysts.[a]

Catalyst	Amounts ($\times 10^{-5}$ mol)	Adipic Acid ($\times 10^{-4}$ mol)	Ketone ($\times 10^{-4}$ mol)	Alcohol ($\times 10^{-4}$ mol)	Time (hr)
$Ru(dmpphen)_3Cl_2$[b]	1.76	2.4	5.0	2.2	43
$Mn(dpphen)_3Cl_2$[b]	0.88	trace	trace	trace	20
$Fe(dmpphen)_3(Otf)_2$[b]	0.88	0	0	0	5
$Co(CH_3COO)_2$	8.8	0	0.94	trace	6
Fe-porphyrin[c]	0.88	0	11.6	2.9	3
Co-nap[d]	0.88	0	8.9	0	6
$Ru(dpphen)_3Cl_2$[e]	0.88	0	0	0	6
$Fe(NO_2\text{-}phen)_3(Otf)_2$[b, d]	0.88	0	8.9	0	6
$Fe(phen)_3(Otf)_2$[b, d]	0.88	0	6.4	0	6
$Fe(dpphen)_3(Otf)_2$[f]	0.88	3.6	18.4	6.3	6
$Fe(dpphen)_3(Otf)_2$	0.88	2.5	7.6	3.7	6

[a] The oxidation reactions were carried out in a 250 mL glass bottle reactor. The reactions consisted of the following: catalyst (8.8×10^{-6} mol), o-dichlorobenzene (10 mL), cyclohexane (5 mL). The pressure apparatus was placed into a constant temperature oil bath at 120 °C and pressurized with 45psi of air. Reactions were run for 6 hours.

[b] Catalyst generated *in situ*

[c] Fe-porphyrin = iron(III) tetra-(pentafluorophenyl) porphyrin chloride, Co-nap = cobalt naphthenate, dpphen = 4,7-diphenyl-1,10-phenanthroline, dmpphen = 2,9-dimethyl-4,7-diphenyl-1,10-phenanthroline. NO_2-Phen = 5-nitro-1,10-phenanthroline; phen = 1,10-phenanthroline, Otf = triflate ($CF_3SO_3^-$)

[d] 10 mL CH_3CN was used instead of 10 mL o-dichlorobenzene as solvent. 30 psi air

[e] Compound provided by Dr. K. S. Schanze, Department of Chemistry, University of Florida.

[f] Oxygen enriched experiment. 35psi air + 10psi O_2

(24 hours) was observed Samples of the commercial catalysts,[41] cobalt naphthenate and cobalt(II) acetate, were tested and found to be inactive for making adipic acid under our reaction conditions

Conclusions

A chemical process has been developed for the catalytic, single step conversion of cyclohexane to solid adipic acid These novel transition metal catalysts, which has high solubility in the aprotic cyclohexane / *o*- dichlorobenzene solution, offers a new way for selective oxidation with dioxygen The good reactivity of the catalysts and the mild reaction conditions in non-acidic solvents may offer an alternative, environmentally friendly process for adipic acid synthesis

CHAPTER 3

ACTIVATION OF HYDROGEN PEROXIDE BY MIXED LIGAND IRON (III) COMPLEXES FOR THE SELECTIVE OXIDATION OF HYDROCARBONS

Introduction

The use of dioxygen for the selective functionalization and oxidation of organic substrates is one of the most challenging and technologically important problems in chemistry. The autoxidation of saturated hydrocarbons under mild conditions is an intellectually challenging and industrially important objective.[42] Designing an oxidation system for saturated hydrocarbons will lead to new opportunities in the chemical process in industry.

The selective hydroxylation of an unactivated carbon-hydrogen bond in nature by use of enzymatic systems such as the iron porphyrin-based cytochrome P-450 clearly indicates that such a process exists.[43] Over the years, enormous research work has been done in this area in order to find a good catalytic system, which has both good reactivity and selectivity for hydrocarbon oxidations. The Gif system is well known in this area and started a new chapter in selective hydrocarbon activation chemistry.[44]

In 1983, Barton first reported a new procedure for the oxidation of saturated hydrocarbons later known as the Gif system.[44a] A typical Gif reaction system contains elemental iron, sodium sulfide, acetic acid, pyridine, and the hydrocarbon substrate. Elemental iron functions not only as a source of metallic cation but also as a reducing agent, and sulfide is used as a ligand for iron. The primary role of pyridine is to trap radicals and acetic acid is used as a proton source (Equation 3.1).

$$\text{Hydrocarbon} + O_2 \xrightarrow[\text{CH}_3\text{COOH, RT}]{\text{Fe, Na}_2\text{S, Pyridine}} \text{Ketone} + \text{Alcohol} \quad (3.1)$$

This basic system is relatively unaffected by the order of mixing of the components. Significantly, the yields can also be obtained with other acids or alkali metal sulfides. The choice of solvent is crucial in controlling not only the yields but also the distribution of the products. The results of oxidation of adamantane by the Gif system clearly shows the oxidation process is not radical reaction in nature, which usually predominantly from the tertiary products and leads to the relative ratio of secondary products to tertiary products of adamantane (C_2/C_3) less than 0.1. Various saturated hydrocarbons, such as admantane, cyclohexane, methyl-cyclohexane, 2 methyl butane and cyclooctane, have been regioselectively oxidized with surprising efficiency by the Gif system.

A trinuclear iron(II), iron(III) complex bridged by carboxylates has been successfully isolated from the Gif system (Figure 3.1). The oxidation results demonstrate not only that the cluster is an efficient catalyst but also that it is superior to the often-employed porphyrin and salen models.[45]

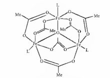

Figure 3 1. Structure of $Fe^{II}Fe^{III}_2O(OAc)_6(Py)_{3.5}$ trinuclear carboxylate cluster

After these first attempts, Gif chemistry moved forward and different systems were developed. All of them have the same chemical peculiarities The nomenclature is geographically based (Table 3.1) G stands for Gif sur Yvette O is for Orsay Agg is for Aggieland (Texas A & M)

Table 3.1 The nomenclature of Gif chemistry [44a]

System	Catalyst	Electron source	Oxidant
Gif^{III}	Fe(II)	Fe^0	O_2
Gif^{IV}	Fe(II)	Zn^0	O_2
GO	Fe(II)	cathode	O_2
$GoAgg^{I}$	Fe(II)		KO_2/Ar
$GoAgg^{II}$	Fe(III)		H_2O_2
$GoAgg^{III}$	Fe(III)/picolinic acid		H_2O_2

After the first significant Gif system (Gif^{III}) had been invented, results showed that the reaction could be made catalytic in iron (up to 2000 turnover) by using metallic zinc as a source of electrons (Gif^{IV}) [46] Hydrogen sulfide was not needed for Gif^{IV} nor for Gif^{III} if the temperature was raised to 40 °C to start the reaction.

An electrochemical version of the Gif system was developed at Orsay Hence, it becomes known as the GO system [47] Coulombic yields can be reached as high as 60% and oxidation yields attained nearly 20%

Fe(II) and peroxide (as KO_2) were used in the GoAgg^{I} system to emulate the peculiar properties of Gif^{IV} system However, the reaction was only theoretically important since it was no preparative value [48] Instead, the GoAgg^{II} system is much more important. Fe(II) and hydrogen peroxide in pyridine/acetic acid also shows the characteristics of Gif-type reactions and up to 30% hydrocarbon activation could be achieved at quantitative yield [49]

One inconvenience of GoAgg^{II} reaction was its relative slow rate. The discovery by Sawyer and co-workers that catalytic amounts of picolinic acid and congeners decrease the reaction half-life from 4-6 hours to 5-10 minutes led to the GoAgg^{III} system (Figure 3 2) [50]

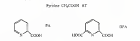

Figure 3 2: GoAgg^{III} system for the oxidation of hydrocarbons

One of the unknown features of Gif chemistry is the mechanism of the ketonization reaction.[44a] A mechanistic scheme (Figure 3.3) shows ketones are not reduced to alcohols under the reaction conditions, and alcohols are not converted to ketones in typical Gif chemistry. This observation suggested that a common reaction intermediate B was responsible for the formation of both ketones and alcohols. Also, mono-substituted alkyl derivatives were found as products by the addition of different trapping reagents to the Gif system. For example, adding $CBrCl_3$ affords to the formation of alkyl bromide. All these results suggest the participation of another reaction intermediate A prior to B, which can be trapped by a trapping reagent.

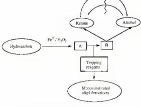

Figure 3.3. Possible mechanism for the Gif chemistry

Another unclear thing is that the rate for oxidizing saturated hydrocarbons to ketones at a faster rate than transforming other easy to oxidize compounds. H_2S, Ph_2S, PPh_3 do not inhibit the reaction although all of these compounds are more easily oxidized than saturated hydrocarbons.

Although great progress has been made in the selective oxidation hydrocarbons by the Gif system, there is still some drawback i.e. low reactivity and short lifetime of the catalyst. For example, the reaction efficiency for the oxidation of cyclohexene at room temperature by using the most active catalyst reported in the literature, Fe-DPA, is only about 30% in 4-6 hours.[5a] The major goal for our work is to improve the well established Gif system especially by increasing the reaction efficiency and the lifetime of the catalyst.

Experimental

Reagents and Equipment

Unless otherwise stated, all reagents were obtained from commercial sources and used without further purification. All solvents were distilled and stored over 4Å molecular sieves before use. Gas chromatographic analyses on volatile products and reactants were carried out by using a Hewlett Packard model 5890 gas chromatograph equipped with Hewlett Packard 50+ column (crosslinked 50% phenyl methyl – 30 m × 0.53 mm × 1.0 μm film thickness) and, helium as the carrier gas, a flame ionization detector, and a Hewlett Packard 3396 Series II integrator. Substrates and products were identified via comparisons with known standards. Calibration curves were used to relate peak areas to the number of moles of products and reactants. Infrared spectroscopy was performed on a Nicolet 5PC equipped with 1MW He-Ne laser and Nicolet PCIR software

(Version 3.2). ^1H and ^{13}C NMR spectra were obtained on a Gemini-300 spectrometer. Elemental analysis data and mass spectra (MS) were performed by spectral services at the University of Florida.

Preparation of $[Fe^{III}(DPA)(H_2O)_3][Fe^{III}(DPA)_2] \cdot 6H_2O$

The title compound[51] was prepared by the following procedure. 30 mL of an aqueous solution (pH = 1.5) containing 10^{-3} mol of $FeCl_3 \cdot H_2O$ and 2×10^{-3} mol of $DPAH_2$ were stirred at room temperature for one hour. After allowing the solution to stand four days, green crystals formed and further used for X-ray crystal structure determination. The crystals decompose when exposed in the air and lose three moles of water for each mole of iron complex. Anal. Calc. for $[Fe^{III}(DPA)(H_2O)_3][Fe^{III}(DPA)_2] \cdot 3H_2O$ ($C_{21}H_{21}N_3Fe_2O_{18}$): C, 35.27, H, 2.96, N, 5.88. Found: C, 35.23, H, 2.84, N, 5.82. Mass FAB: m/e: 367, 331, 314, 275, 239

Preparation of $Fe_2^{III}(DPA)_2(O_2) \cdot 3H_2O$

An appropriate amount of $Fe^{III}(DPA)(OH)(H_2O)_{1.5}$ complex (~0.5g) was dissolved in ethanol solution at 0°C. Excess amounts H_2O_2 (50%) were slowly added. The solution was stirred at 0°C for 2 hours. A red precipitation was generated. The solid product was separated and dried in vacuum oven at room temperature for 5 hours (yield 30%). Elemental analysis data for $Fe_2^{III}(DPA)_2(O_2) \cdot 3H_2O$ ($Fe_2C_{14}H_{12}N_2O_{13}$). Found (%): C, 31.74, H, 2.44, N, 5.24. Calculated (%): C, 31.85, H, 2.29, N, 5.31

Isolation of $Fe^{III}(DPA)(DPAH)(Py)$

An appropriate amount of $Fe^{III}(DPA)(OH)$ catalyst (~0.5g) was added to a mixed solution containing 5 mL pyridine, 2 mL acetic acid and 0.5 mL cyclohexene. Hydrogen peroxide (~0.1 mL 35% H_2O_2) was slowly add to the reaction and reactions were run at

25 °C A pale green precipitation was generated The solid product was separated by filtration and further washed with CH_3CN and dried in vacuum oven at 70 °C for overnight (yield 65%) Elemental analysis data for Fe^{III}(DPA)(DPAH)(Py) ($Fe_1C_{16}H_{12}N_3O_8$) Found (%) C, 48 60, H, 2 55, N, 8 85 Calculated (%) C, 48 95, H, 2 59, N 9 01 MS-ESI MW = 388 for $[FeIII(DPA)(DPAH_2)]^+$

Preparation of Fe(III)-DPA Complexes with Various Ligands

The compounds, Fe^{III}(DPA)(DPAH), Fe^{III}(DPA)(Cl), Fe^{III}(DPA)(μ- OH) Fe^{III}(DPA)(Phen)Cl, Fe^{III}(DPA)(AcAc), were made by literature methods [52]

Preparation of $Fe^{III}(DPA)(OH)(H_2O)_{0.5}$

The complex $Fe^{III}(DPA)(OH)(H_2O)_{0.5}$ was synthesized as follows $DPAH_2$ was neutralized by two equivalent of triethylamine in acetonitrile solution. After adding $Fe(ClO_4)_3$, a pale green precipitation was generated The solid product was further washed with CH_3CN and dried in vacuum oven at 70 °C for overnight (yield 70%) Elemental analysis data for $Fe^{III}(DPA)(OH)(H_2O)_{0.5}$ ($C_7H_5N_1O_{5.5}Fe_1$) C 34 04, H 2 04, N 5 67%, found C 34 00, H 2.22, N 5.55%

General Procedure for the Oxidation of Hydrocarbons by Hydrogen Peroxide

The appropriate amount of catalyst was added to a mixed solution containing 5 mL pyridine, 2 mL acetic acid and hydrocarbon Hydrogen peroxide was slowly add to the reaction, and reactions were run at 25 °C Reactant consumption and reaction products were monitored and quantified by GC The moles of each of the reactants and the known products were determined using calibration curves for each compound

Determination of the crystal structure of $Fe^{III}(DPA)(H_2O)_3][Fe^{III}(DPA)_2]\cdot 6H_2O$

X-ray crystallography work was done by Dr K. A. Abboud at the Department of Chemistry, University of Florida. The main parameters for the structure determination are listed below (Table 3.2)

Table 3.2 Main parameters for $Fe^{III}(DPA)(H_2O)_3]$ $[Fe^{III}(DPA)_2]\cdot 6H_2O$

Siemens P3/PC diffractometer	4326 reflections with $I > 2\sigma(I)$
ω scans	$R_{int} = 0.015$
Absorption correction: by integration	$\theta_{max} = 25°$, $h = 0\text{-}10$, $k = -13\text{-}13$,
based on measured crystal faces[53]	$l = -19\text{-}19$ 4 standard reflections every
$T_{min} = 0.638$, $T_{max} = 0.783$	100 reflections intensity decay < 1%
5714 measured reflections	5323 independent reflections
$R[F^2 > 2\sigma(F^2)] = 0.035$	$(\Delta/\sigma)_{rms} = 0.001$
$WR(F^2) = 0.097$	$\Delta\rho_{max} = 0.568$ e Å^{-3} $\Delta\rho_{min} = -0.566$ e Å^{-3}

Results and Discussion

Crystal Structure of $Fe(C_7H_3N_1O_4)(H_2O)_3]$ $[Fe(C_7H_3N_1O_4)_2]\cdot 6H_2O$

The crystal data are listed in Table 3.3 and the selected bond lengths are shown in Table 3.4

Table 3.3 The crystal data for $[Fe(C_7H_3N_1O_4)(H_2O)_3]$ $[Fe(C_7H_3N_1O_4)_2]\cdot 6H_2O$

$M_r = 769.14$	Mo K_α radiation, $\lambda = 0.71073$ Å
Cell parameters from 40 reflections	Triclinic, P
$a = 8.582$ (2), $b = 11.313$ (2), $c = 16.251$ (3)Å	$\theta = 10\text{-}11°$, $\mu = 1.056$ mm^{-1}
$\alpha = 74.75$ (3), $\beta = 87.29$ (3), $\gamma = 83.16$ (3)°	$V = 1511.2$ (5) Å^3 $Z = 2$
Prism, $0.57 \times 0.43 \times 0.27$ mm. Green	$T = 293$ (2) K
$D_x = 1.690$ Mg m^{-3}	D_m not measured

Table 3.4 Selected bond lengths (Å)

Fe1-O15	1.971 (2)	Fe2-O8A	2.025 (2)
Fe1-O16	2.004 (2)	Fe2-O8	2.028 (2)
Fe1-O17	1.987 (2)	Fe2-O14A	2.023 (2)
Fe1-O1A	2.119 (2)	Fe2-O14C	2.023 (2)
Fe1-O7A	2.108 (2)	Fe2-N2	2.054 (2)
Fe1-N1	2.059 (2)	Fe2-N2	2.054 (2)

The reaction of iron with dipicolinic acid (2,6-pyridinedicarboxylic acid) is much more complicated than expected, particularly in the solid state. Several crystal structures of iron(III) and iron(II) complexes with $DPAH_2$ and its derivatives have been reported in which mononuclear, binuclear and polynuclear structures are formed. The ligand to iron ratio can be one or two, six and seven coordinate iron complexes result.[53, 54] Interest in this area stems from the biological activity of dipicolinic acid for enhancing production of spore photoproducts in bacterial spores upon UV irradiation,[55] the usefulness of dipicolinic acid in analytical chemistry for the determination of iron[56] and the catalytic activity of iron-dipicolinate complexes for the activation of dioxygen and hydrogen peroxide.[57] We synthesized and determined the crystal structure of complex, (**I**)

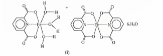

(**I**)

The asymmetric unit consists of an $[Fe(C_7H_3N_1O_4)(H_2O)_3]^+$ cation, an $[Fe(C_7H_3N_1O_4)_2]$ anion and six water molecules of crystallization Each of the Fe atoms has an octahedral coordination geometry, which is distorted due to the structural requirements of the tridentate dipicolinate ligands The two ligands in the complex anion are *trans* meridional with respect to each other and have a dihedral angle of 93 74 (6)° All three ligands are nearly individually planar, with the largest deviations observed in the positions of the carboxylic O atoms These deviations can be described by a slight rotation of each carboxylate group from its respective ligand with angles ranging from 1 1 (3)° for the C1 group to 3 9 (4)° for the C7 group The Fe-O bonds are comparable in both ions [distances range from 2 008 (2) to 2 028 (2) Å] and are equivalent to Fe^{III}-O bonds in other Fe^{III}(DPA) complexes [52, 54] However they are short than their counterparts in Fe^{II}(DPA) complexes Observed Fe^{II}-O distances are in the range of 2 137 (6) to 2 213 (6) Å [52a, b] On the other hand, the Fe-N bonds are equal in both ions [2 059 (2) Å in the cation and 2 054 (2) Å for each bond in the anion], and they are equivalent to Fe^{III}-O and Fe^{II}-N bond lengths in similar complexes The shorting of the Fe-O distance with the Fe-N distance remaining unchanged cannot be explained by the smaller ionic radius of Fe^{III} compared with Fe^{II} for this would lead to shortening of both Fe^{III}-O and Fe^{III}-N bonds. A search of the April 1997 release of the Cambridge Structural Database revealed that Fe^{II} and Fe^{III} have bonds to pyridinium N atoms in the wide range of 1 90 to 2 75 Å.

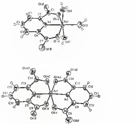

Figure 3.4: Crystal structure of $[Fe(C_7H_3N_1O_4)(H_2O)_3]$ $[Fe(C_7H_3N_1O_4)_2]\cdot 6H_2O$

All available protons are involved in an extensive three-dimensional network of hydrogen bonding. Although the H atoms of the distordered O23 and O23' partial water molecules were not found these molecules are also involved in hydrogen bonding.

Mixed Ligand Fe(III) Complexes for the Oxidation of Hydrocarbons in Gif System

When we run a Gif type of reaction using $Fe^{III}(DPA)(OH)$ as catalyst, precipitation was found in the reaction system after several hours. One iron complex can be carefully isolated and the results from element analysis and MS-ESI indicates the precipitation is $Fe^{III}(DPA)(DPAH)(Py)$. It is reasonable to suggest that the catalyst deactivated by the formation of precipitation because the oxidation reaction stops after 4-6 hours even with significant amounts of hydrocarbon and hydrogen peroxide left in the reaction system.

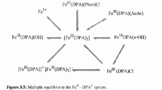

Figure 3.5: Multiple equilibria in the Fe^{III}–DPA^2 system.

Dipicolinate (DPA^{2-}) is a very labile ligand when coordinated to Fe^{III}. As shown in Figure 3.5, multiple equilibria can be expected. Different kinds of Fe^{III} complexes can be formed even by slightly changing the system conditions such as pH, solvent, the ratio of Fe^{III} to DPA^{2-}, other potential ligand existing in the solution, *etc.* The concentration of the active iron species will decrease or even be depleted during the reaction process.

Stabilizing the catalyst may increase the lifetime and reactivity of the iron catalyst, several mixed-ligand iron complexes were synthesized and one of them we determined the crystal structure.

Table 3.5 summarized all the results of cyclohexene oxidation by different iron compounds (Equation 3.2), which we isolated or generated *in situ*. The reaction conditions are the same as reported in the literature in order to allow a comparison.[50a] The data in the entry **1** is the best result in the literature.[50a] Comparing with the data from entry **2** to entry **1**, there is no reactivity difference when we using Fe^{III} instead of Fe^{II} with the same ligand. This also shows the catalytic cycle is independent of the initial oxidation state.

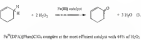

(3.2)

Fe^{III}(DPA)(Phen)ClO_4 complex is the most efficient catalyst with 44% of H_2O_2 utilized for cyclohexene transformation in 4 hours. Again, comparing with the best result listed in the entry **1** that has 26% efficiency, our catalyst is at least 70% more active than the previous one. One more interesting result is that the two complexes listed in entry **4** and entry **5** have same chemical composition but may have different structures. The hydroxyl-bridged complex Fe^{III}(DPA)(μ-OH) has less reactivity. The structure difference has great influence on the reactivity. All of the reactions listed in Table 3.5 show the typical Gif type of chemistry, where ketone is formed as a major product. No 2-cyclohexen-1-ol and cyclohexene oxide are detected within GC detection limit.

Table 3.5. Oxidation of cyclohexene by iron complexes [a]

Entry	Catalyst (mM)	-One (mM)	Time (hr)	H_2O_2 Eff (%)
1	$[Fe^{II}(DPA)_2]^{2-}$ [b]	13	4-6	26
2	$Fe^{III}(DPA)(DPAH)$	14	4	28
3	$Fe^{III}(DPA)(Cl)$	11	4	22
4	$Fe^{III}(DPA)(OH)$	12.4	4	25
5	$Fe^{III}(DPA)(\mu\text{-}OH)$	9	4	18
6	$Fe_2^{III}(DPA)_3(H_2O)_3$	5.6	4	11.2
7	$Fe^{III}(DPA)(Phen)ClO_4$ [c]	22	4	44
8	$Fe^{III}(DPA)(Phen)Cl$	19	4	38
9	$Fe^{III}(DPA)(DIP)ClO_4$ [d]	19	4	38
10	$Fe^{III}(DPA)(DMP)Cl$ [c]	6.4	4	12.8
11	$Fe^{III}(DPA)(AcAc)$	14	4	28
12	$Fe^{III}(TPy)(AcAc)$ [c]	5	4	10

[a] The reaction consisted as following 5 mM catalyst, 1 M cyclohexene, 100 mM H_2O_2 5 mL pyridine, 2 mL acetic acid Reactions were run at 25 °C

[b] Data was got from reference [50a]

[c] Complexes generated *in situ*

[d] DIP = 4,7-diphenyl-1,10-phenanthroline DMP = 2,9-dimethyl-1,10-phenanthroline AcAc = 2,4-pentanedione Tpy = 2,2,'6,2' terpyridine

Different kinds of hydrocarbons can be oxidized by using Fe(DPA)(Phen)(Cl) as catalyst (Table 3.6) Ethylbenzene is the most reactive hydrocarbon and we observed 82% H_2O_2 efficiency and 16 turnovers in 4 hours Adamantane has 12 equivalent of secondary C-H and 4 equivalent of tertiary C-H If all positions have same reactivity towards the oxidation, the C2/C3 ratio for the oxidation products should be equal to 3. If there is a radical reaction, which is preferentially goes to tertiary carbon, the C2/C3 ratio is about 0.05-0.15.[44c] The C2/C3 ratio we found for oxidation of adamantane is 2.8, which suggests a non-radical mechanism.

Table 3.6 Activation of H_2O_2 by Fe^{III}(DPA)(Phen)Cl for the oxygenation of hydrocarbons [a]

Substrate	H_2O_2 Eff (%)	Products	TON
Cyclohexene	38	cyclohexenone	8
Cyclohexane	68	cyclohexanone	14
Pentane	38	2-pentanone 71%, 3-pentanone 29%	8
$PhCH_2CH_3$	82	$PhC(O)CH_3$ 97%, $PhCH(OH)CH_3$ 3%	16
$PhCH_3$	34	PhCH(O) 45%, $PhCH_2(OH)$ 36%, *p*-$(HO)PhCH_3$ 19%	7
Adamantane	36	2-adamantanone 74%, 1-adamantanol 26%, trace 2-adamantanol	7

[a] The reactions consisted as following: 5 mM catalyst, 1 M cyclohexene, 100 mM H_2O_2, 5 mL pyridine, 2 mL acetic acid. Reactions were run at 25 °C for 4 hours.

We ran several experiments in order to gain a deeper understanding of the mechanism of the reaction. The results are listed in Table 3.7. The cyclohexanol oxidation reaction indicates the formation of cyclohexanone does not go through cyclohexanol as intermediate. There is not a large isotope effect because the reaction rate for the oxidation of d_{12}-cyclohexane is almost equal to that of normal cyclohexane. Adding radical inhibitor, BQ (benzoquinone) and radical initiator, AIBN (2,2'- azobisisobutyronitrile), did not affect the reaction rate, which supports a non-radical mechanism

Table 3 7. Study on the mechanism of the oxidation reaction [a]

Substrates	H_2O_2 Eff (%)	Products	TON
Cyclohexanol (21mM)	0 7	cyclohexanone	–
Cyclohexane	42	cyclohexanone	8
d_{12}-cyclohexane	35	d_{10}-cyclohexanone	7
Cyclohexene	21	cyclohexenone	4
Cyclohexene + BQ (5mM)	20	cyclohexenone	4
Cyclohexene + AIBN (5mM)	22	cyclohexenone	4

[a] The reaction consisted as following 0 5 mM Fe^{III}(DPA)(Phen)Cl, 1M substrate, 100 mM H_2O_2 5 mL pyridine, 2 mL acetic acid. Reactions were run at 25 °C for 1 hour BQ = 1,4-Benzoquinone. AIBN = 2,2'-Azobisisobutyronitrile.

Isolation of the Active Intermediate in Gif System

Recently, a μ-peroxo-dimer was found to be an intermediate in the catalytic cycle of MMO oxidations.[57] After adding H_2O_2 in the solution when we use Fe^{III}(DPA)(OH) as catalyst, the solution changes color from pale green to red Our speculation is that it may form some kind of intermediate Isolation this intermediate may lead to better understanding the mechanism of Gif chemistry In the literature, the formation of iron peroxo intermediate in the Gif system was suggested but has not been isolated [50d, 58] Based on our experimental results one example of the proposed Fe^{III}-μ-peroxo-dimer, $Fe_2^{III}(DPA)_2(O_2)3H_2O$ can been successfully isolated as depicted in Figure 3 6

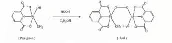

Figure 3 6· Isolation of the Fe^{III}-μ-peroxo-dimer

Comparing with the original IR spectra for Fe^{III}(DPA)(OH) the μ-peroxo-dimer shows a new band at 870 cm^{-1}, which is in the normal O-O stretching region (790-930 cm^{-1})[59] The new μ-peroxo-dimer compound is relatively stable in the solid state but unstable in the liquid state Attempts to grow X ray quality crystals were unsuccessful

The evidence form the NMR spectra also support the formation of the iron (III) μ-peroxo-dimer Because the electron spin moment is so large for paramagnetic complex, a broad NMR spectrum will be observed and all the peaks are shifted. That is exactly what we found on the ^{1}H NMR spectrum of Fe^{III}(DPA)(OH) When two iron(III) ions are bridged by O-O group and form the μ-peroxo-dimer, the antiferromagnetic coupling between the two iron(III) greatly reduce the paramagnetism of the iron complex All NMR peaks are much sharper (Figure 3 7)

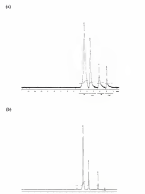

Figure 3.7: ^{1}HNMR spectra of **Fe^{III}**(DPA)(OH) **(a)** and Fe$_2^{III}$(DPA)$_2$ (O$_2$)·3H$_2$**O (b)**

By using the isolated compound we can oxidize cyclohexane to cyclohexanone in the same reaction conditions we used before (Figure 3.8). The instability of the intermediate in the solution may cause the low efficiency of the reaction (~15%)

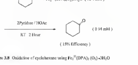

Figure 3.8 Oxidation of cyclohexane using $Fe_2^{III}(DPA)_2\,(O_2)\bullet 3H_2O$

Conclusions

Several mixed ligand iron (III) complexes were synthesized. The crystal structure of $[Fe(C_7H_3N_1O_4)(H_2O)_3]\,[Fe(C_7H_3N_2O_4)_2]\bullet 6H_2O$ was determined. $[Fe^{III}\,(DPA)(Phen)ClO_4]$ complex is the most efficient catalyst and is at least 70% more active than the previous best catalyst $[Fe^{II}DPA)_2]$ in the literature. Several experiments indicate that the reaction is occurring via a non-radical mechanism. An iron (III)-peroxo reactive intermediate was successfully isolated. This complex reacted with cyclohexane to give solely cyclohexanone with 15% efficiency in two hours

CHAPTER 4
ENANTIOSELECTIVE EPOXIDATION CATALYZED BY MANGANESE SCHIFF BASE COMPLEXES

Introduction

Epoxidation, which is the addition of a single oxygen atom to a carbon-carbon double bond, is an important reaction in the field of organic synthesis. Epoxides are useful intermediates that can be converted to a variety of organic compounds.[60] In particular, chiral epoxides have the potential to serve as building blocks in the synthesis of natural products, and enantioselective epoxidation of simple olefins represents a challenging synthetic problem. The increasing demand for enantiomerically pure pharmaceutical compounds[61] has fueled the search for asymmetric epoxidation catalysts that can introduce one or two new stereocenters upon reaction with an olefin of appropriate symmetry. Several studies of reactions with exogenous olefins have shown that P-450 enzymes can perform asymmetric epoxidation with high enantioselectivities. Although nature has provided an obvious impetus for the creation of effective biomimetic metalloporphyrin catalysts, the vital chemical importance of enantioselective epoxidation has driven the exploration of more non biological systems.

In 1965, British chemist H. B. Henbest first reported an asymmetric epoxidation process.[62] The asymmetric agent used was a chiral peracid. A brief glance at the mechanism for these epoxidations (Figure 4.1) reveals that it was a less efficient system for realizing asymmetric induction in the oxygen transfer step. The line of approach of the alkene is about four bond lengths away from the chiral group (R*) and the observed asymmetric introductions were poor. Nevertheless, this was the first asymmetric epoxidation and an important beginning.

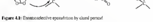

Figure 4.1: Enantioselective epoxidation by chiral peracid

The extremely effective Sharpless asymmetric epoxidation catalysts were introduced in the early 1980's. Sharpless epoxidation system consists a mixture of commercially available titanium(IV) tetraisopropoxide, TBHP, and (+)- or (-)-diethyl tartrate that effectively facilitates enantioselective epoxidation of allylic alcohols with a high enantiomeric excess (ee) value (up to 99% ee).[63] The relatively slow reaction can be accelerated by the addition of 3-4Å molecular sieves.[64]

With (-)-diethyl tartrate the oxidant approaches the allylic alcohol from the top plane whereas the bottom side is accessible to the (+)-diethyl tartrate reagent, giving rise to the corresponding optically active alcohol (Figure 4.2)

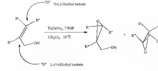

Figure 4.2. Sharpless epoxidation reaction.

The structures of several catalytically active titanium-tartrate complexes have been determined by X-ray crystallographic methods.[65] These results revealed that the titanium tartrate complexes are at least dimeric. Based on this information, attempts have been made to explain the mechanism of these asymmetric epoxidations from both an experimental[55a] and a theoretical[66] point of view. It has been suggested that the axial and equatorial ligands undergo an exchange with a bidentate coordinated peroxide and that the axially coordinated carbonyl is released from the titanium center and substituted by the allylic alcohol. A model in which the peroxide bond is nearly perpendicular to the equatorial plane appears to be the least sterically hindered, which results in a linear alignment of allylic alkoxide and peroxide oxygen atoms and a roughly octahedral titanium coordination geometry as shown in Figure 4.3.

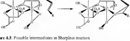

Figure 4.3: Possible intermediates in Sharpless reaction

A theoretical approach to the mechanism for the Sharpless asymmetric epoxidation shows that when the orientation of the allylic alcohol around the peroxygens is varied, no electronic origin for the high enantioselectivity is found.[65] The steric effects associated with the three-dimensional chiral nature of the catalyst are largely responsible for the transfer of the oxygen to a specific enantioface of the allylic alcohol. An extended Hückel investigation of the electronic structure of the titanium-tartrate catalysts showed that the coordination of one tartrate carbonyl moiety to the axial position of the titanium atom leads to a preference of the other tartrate group to coordinate *trans* to the titanium-coordinated carbonyl group, leaving two vacant sites for bidentate coordination of the peroxide.[66a]

The Sharpless asymmetric epoxidation catalyst has already shown its efficiency in the synthesis of natural products.[67] However, these epoxidations are limited to that of functionalized olefins.[63a] The new challenge is to develop a system that will have high enantioselectivities via nonbonding interactions. The development of chirally modified metalloporphyrins by the group of Groves, Mansuy and Kodadek provided another transition metal-catalyzed entry to optically active epoxides.[68] Asymmetric epoxidation of prochiral olefins with ee of up to 72%, such as β-methyl styrene, was achieved by using chiral metalloporphyrins as catalysts. The inherent sensitivity of the porphyrins to oxidation can be reduced by skillful substitution of the *meso* phenyl groups, making higher turnover numbers in catalytic processes possible.

Recently, an important catalytic system that utilized chiral manganese salen complexes with good enantioselectivity in the epoxidation of nonfunctionalized olefins was discovered by Jacobsen and Katsuki independently.[69] Salens, like porphyrins, usually bind transition metals with a square-planar configuration. Kochi and coworkers showed that achiral Mn(III)salen complexes catalyze the epoxidation of olefins in the presence of a stoichiometric oxidant.[70] As in metalloporphyrin systems, the reactive species in metallosalen oxidations is probably a high-valent metal-oxo complex. Asymmetric metallo-salen catalysts offer an advantage over chiral porphyrin systems because the salen ligand has two chiral sp^3-hybridized carbon atoms at its periphery (Figure 4.4). Because these chiral carbon atoms are just two bond lengths away from the metal, their proximity to the reactive site allows a high degree of stereoselectivity.

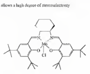

Figure 4.4 One example of a Jacobsen Katsuki catalyst

Since the first report of asymmetric catalysis with chiral Mn(III)salen complexes by Jacobsen and co-workers,[71] more than 120 chiral Mn(III)salen derivatives have been studied as catalysts for the epoxidation of a variety of unfunctionalized olefins with iodosylarenes, sodium hypochlorite, or dioxygen as the oxidant. The majority of these systems are derived from chiral 1,2-diamino-1,2-diphenylethane or chiral *trans*-1,2-diaminocyclohexane. Greater than 90% ee can be obtained in the epoxidation of various *cis*-disubstituted olefins. Facile and relatively inexpensive ligand syntheses, coupled with high enantioselectivities and the ability to use a cheap stoichiometric oxidant, make these the best practical catalysts currently available for epoxidizing unfunctionalized olefins. Merck currently synthesizes antihypertensive chromanol derivatives with one of the Jacobsen-Katsuki catalysts and hypochlorite.[67b]

A modified Jacobsen-Katsuki catalytic system was developed by using an achiral manganese(III)salen complex with a chiral amine. These results support the proposal that the a non planar and chiral structure of the salen ligand plays an important role in the enantioface selection of olefins by manganese(III)salen complex.[72] Generally, H_2O_2 is not a good oxidant with Jacobsen-Katsuki catalysts because it readily goes through a homolytic cleavage of its week O-O bond to form radicals. However, using a Jacobsen-Katsuki catalyst together with a carboxylate salt as a cocatalyst in the presence of either H_2O_2 or anhydrous urea H_2O_2 gives good yields of epoxides with moderate to excellent enantioselectivity.[73]

Shibasaki *et al.* reported the general and practical catalytic enantioselective epoxidation of enones (α,β-unsaturated ketones) in the presence of Ln-BINOL derivative complexes (Ln = lanthanide; BINOL = 1,1'-bi-2-naphthol)[74] in which 4Å molecular sieves were added to the reaction system to remove water and form the product in high yield. The catalytic asymmetric epoxidation can be carried out at room temperature using 1-8 mol% of a chiral catalyst to give epoxides with good ee (80 95%). Later it was found that with small amounts of water in the reaction system (5 equivalents to catalyst), the enantioselective epoxidation of enones was greatly improved [75] The addition of triphenylphosphine oxide also significantly enhanced the degree of asymmetric induction in the chiral Ln-BINOL complex-catalyzed epoxidation of enones using *tert*-butylhydroperoxide (TBHP) as the oxidant. One example shows the observed ee increase from 73% to 96% ee when chalcone was used as the substrate. The hypothesis is that ligation by $Ph_3P=O$ produces a non-polymeric catalyst having a monomeric structure [76]

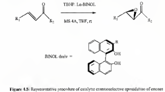

Figure 4.5: Representative procedure of catalytic enantioselective epoxidation of enones promoted by Ln BINOL derivatives

Recently Shi *et al.* reported a highly enantioselective epoxidation method for substituted olefins using a fructose-derived ketone 1 as the catalyst and Oxone as the oxidant (Figure 4.6).[77] High enantioselectivities (> 95% ee) have been obtained for *trans*-disubstituted and trisubstituted olefins, which can have functional groups such as tributylsilyl ether, chloride, and ester. The enantiomeric excesses for *cis*-olefins and terminal olefins are not high.

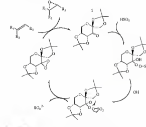

Figure 4.6: Possible reaction pathways of the epoxidation catalyzed by ketone **1**

Although great progress has been made in the preparation of catalysts for the regioselective and enantioselective epoxidation of unfunctionalized olefins, these catalysts are only beginning to be useful synthetic tools. Elaborate and expensive catalyst syntheses as well as low turnover numbers (the typical turnover numbers for Jacobsen-Katsuki catalysts are below 40), both plague each of the systems discussed above to varying degrees. Also, for many catalysts, practical oxidants such as bleach, hydrogen peroxide, *tert*-butylhydroperoxide, or dioxygen fail to give the selectivity or number of turnovers achieved with expensive oxidants such as iodosylbenzene and Oxone. Therefore, searching for cheap, useful, viable enantioselective epoxidation catalysts is still a significant challenge for chemists.

Naturally abundant amino acids are readily available chiral sources and are potential ligands for asymmetric catalytic reactions. However, no systematic work of their use in epoxidation of olefins has been made thus far. Our work is based on the use of transition metal Schiff base complexes that induces chirality via optically pure amino acids. A series of chiral Schiff base complexes derived from amino acids have been synthesized. These complexes were then screened in a variety of epoxidation reaction conditions and evaluated for their ability to induce enantioselective epoxidations.

Experimental

Reagents and Equipment

Unless otherwise stated, all reagents were obtained from commercial sources and used without further purification. All solvents were distilled and stored over 4Å molecular sieves before use. Gas chromatographic analyses on volatile products and reactants were carried out by using a Hewlett Packard model 5890 gas chromatograph equipped with Hewlett Packard 50+ column (crosslinked 50% phenyl methyl – 30 m × 0.53 mm × 1.0 μm film thickness), helium as the carrier gas, a flame ionization detector, and a Hewlett Packard 3396 Series II integrator. A cyclodextrin B 30 m capillary column (J & W Scientific) was used to determine the ee value of the epoxide. Substrates and products were identified via comparisons with known standards. Calibration curves were used to relate peak areas to the number of moles of products and reactants. Column chromatorgraphy and flash column chromatorgraphy were performed using 60Å, 200-425 mesh silica packed in glass columns. Infrared spectroscopy was performed on a Nicolet 5PC equipped with 1MW He-Ne laser and Nicolet PCIR software (version 3.2). ^{1}H and ^{13}C NMR spectra were obtained on a Gemini-300 spectrometer. Elemental analyses were performed at the University of Florida.

Preparation of Manganese(II) Salicylidene (L-A.A) (A.A = Phenylalanine, Tryptophan)

These compounds were made by a modified literature method.[78] Five mmol of L-amino acid was refluxed with an equal amount of salicylaldehyde in 50 mL of degassed 3:1 ethanol / water under a nitrogen atmosphere for 2 hours. An equal number of millimoles of $Mn(Ac)_2 \cdot 4H_2O$ were then added. Further stirring for approximately 3-4 hours gave a large crop of yellow product. The precipitate was then washed three times with small quantities of above solvent and dried in a vacuum oven at 60 °C for at least 12 hours. A yellow powder was obtained as the final product. Element analyses. Found for Mn^{II} (Sal-L-Phe) $1.5H_2O$: C, 57.97%, H, 5.09%, N, 3.87%. Calculated: C, 57.67%, H, 4.84%, N, 4.20%. Element analyses: Found for Mn^{II} (Sal-L-Try) $1.5H_2O$: C, 55.46%, H, 4.04%, N, 6.80%. Calculated: C, 55.65%, H, 4.11%, N, 7.21%.

Preparation of Manganese(III) Salicylidene L- Histidine

Five mmol of L-histidine were refluxed with equal amounts of salicylaldehyde in 50 mL of degassed ethanol under nitrogen atmosphere for 2 hours. An equal number of millimoles of $Mn(Ac)_2 \cdot 4H_2O$ were then added. Further stirring for overnight under an air atmosphere gave a dark brown solution. The solution was cooled in an ice bath and the dark brown precipitate was filtered, washed three times with small quantities of cold absolute ethanol, and dried in vacuum at 60 °C for at least 12 hours. Element analyses Found for Mn^{III} (Sal-L-His) (CH_3COO) C, 41.47%, H, 4.15%, N, 11.11%. Calculated C, 41.71% H, 3.75%, N, 10.42%.

Preparation of Manganese 3,5-*tert*-Butyl-Salicylidene L-Amino Acid (amino acid = tryptophan, histidine)

Five mmol of L- amino acid were refluxed with equal amounts of 3,5-*tert* butyl-salicylaldehyde in 50 mL of degassed ethanol under nitrogen atmosphere for 2 hours. An equal number of millimoles of $Mn(Ac)_2 \cdot 4H_2O$ was then added. After refluxing for approximately 3-4 hours, the solution was exposed to the air and the volume of solution was reduced to 10 mL. 100 mL of water were added to precipitate the brown powder. The precipitate was washed three times with small quantities of above solvent, and dried in vacuum at 60 °C for at least 12 hours. A brown powder was obtained as the final product. Element analyses: Found for Mn(*t* Bu-Sal L-Try) O_2 C, 61.34% H, 5.42%, N, 5.49% Calculated C, 61.78%, H, 5.98%, N, 5.54% Found for Mn(*t* Bu-Sal-L His) O_2 C, 55.43% H, 5.98%, N, 9.10%. Calculated C, 55.27%, H, 5.96%, N, 9.21%

Preparation of Manganese -(S,S)- L-Tryptophan (S,S = 3,5-Br- Salicylaldehyde, 4,6-OCH_3 - Salicylaldehyde, 5-Br- Salicylaldehyde, 3-OH Salicylaldehyde, 4,6-OH Salicylaldehyde)

These series of substituted salicylaldehyde were prepared by using the similar procedures for the preparation of manganese 3,5-*tert* butyl salicylidene L-tryptophan. Element analyses Found for Mn (3,5-Br-Sal L-Try) 0.5C_2H_5OH C, 42.52% H, 2.38%, N, 4.75% Calculated C, 42.10%, H, 2.79%, N, 5.17% Found for Mn (4,6-OCH_3-Sal-L-Try) $2H_2O$ C, 50.38%, H, 4.54%, N, 6.65% Calculated C, 50.36%, H, 4.23% N

6 53% Found for Mn (5-Br-Sal-L-Try) $0.5H_2O$ C, 47 90%, H, 3.39%, N, 5 98% Calculated C 48 13% H, 3 14%, N, 6 24% Found for Mn (3 OH Sal L-Try) $1.5H_2O$ C, 53 41%, H, 3 73%, N, 6 66% Calculated C, 53 48%, H 4.24% N, 6 93% Found for Mn (4,6-OH-Sal-L-Try) $2H_2O$ C, 50 38%, H, 4 54%, N, 6 65% Calculated C, 50 36%, H 4 23%, N, 6 53%

General Procedure for Epoxidation of Styrene with Hydrogen Peroxide

The appropriate amounts of catalyst were added to a mixed methanol and styrene solution. 35% hydrogen peroxide was added during 0 5-1 hour period Cyclohexane (0 1 mL) was added to the above solution as an internal standard The resulting brown solution was stirred at 0°C Reactant consumption and reaction products were monitored and quantified by GC The moles of each of the reactants and the known products were determined using calibration curves for each compound Reaction time was varied between 16-24 hours The reaction products were separated by flash chromatography (silica gel hexanes / diethyl ether 80 20, v / v) to afford a fraction containing styrene oxide Analysis of styrene oxide ^{1}H NMR ($CDCl_3$) δ 2 81 (dd $J_1 = 5.4Hz$ $J_2 = 3.0Hz$, 1H), δ 3 15 (dd $J_1 = 5.4Hz$ $J_2 = 1.5Hz$ 1H) δ 3 87 (dd, $J_1 = 4.2Hz$ $J_2 = 1.5Hz$ 1H) δ 7 33 (m 5H)

General Procedure to Determine Enantiomeric Excess of Epoxide by ^{1}H NMR

A sample of the isolated epoxide (~0 1 mL) was placed in a NMR tube along with tetramethylsilane (~0 1 mL, and dissolved in ~0 5 mL $CDCl_3$). An initial ^{1}H NMR spectrum was taken before ~0 1mL aliquots of a $CDCl_3$ solution containing tris-[3-(heptafluoropropylhydroxymethylene)-(+)-camphorato] europium(III) derivative, [Eu(hfc)$_3$] were added to the NMR sample tube The ^{1}H NMR spectra were monitored for the shift in the doublet of doublets peak at δ 3.15. When the appropriate amount of the $Eu(hfc)_3$ solution was added, the peak would shift downfield and be split into a doublet of triplets. The integration of these two triplet peaks was used to calculate the ee by the following (Equation 4.1)

$$ee = \frac{(\text{Integration of peak 1}) - (\text{Integration of peak 2})}{(\text{Integration of peak 1}) + (\text{Integration of peak 2})} \times 100 \quad (4.1)$$

Results and Discussion

Preparation of Manganese-Salicylidene-Amino Acid Complexes

Lo[79] reported two step syntheses of the manganese-salicylidene-amino acid complexes. Because of the instability of the Schiff base, it is difficult to get pure Schiff base ligands and the subsequent manganese complexes. However, a one-pot synthesis, which uses inert atmosphere techniques allowed for the successful isolation and purification of these complexes. Using 3,5-*tert* butyl-salicylaldehyde as a starting building block instead of salicylaldehyde leads to the increased solubility of the corresponding manganese complexes in the organic solvents. By reducing the volume of the solution and pouring into a large amount of water pure complexes were easily obtained.

It is interesting that these types of complexes bind dioxygen. Although we do not have direct evidence to show such kind of oxygenation compounds exist, fast color change from yellow to brown when the complexes are exposed in air and IR spectra absorption at approximately 793 cm^{-1} presumably from the formation of O_2^{2-} strongly suggest the formation of manganese oxygen compounds.[70] He prepared a series of manganese(II) complexes of Schiff bases derived from salicylaldehyde and amino acids and found the compounds absorbed oxygen readily in many different organic media. The oxygenation compounds can also be partially deoxygenated.[70]

Styrene Epoxidation

The first objective was to find suitable reaction conditions to effectively carry out the epoxidation reactions. After a good system for our catalysts was found enantioselective studies were done. Styrene was used as the model substrate in the epoxidation reactions since it has one prochiral carbon and is inexpensive. The epoxidation products of styrene are also easily identified and separated by GC.

In the initial activity screening of our catalysts, we used the same reaction conditions that Jacobsen used for his catalyst[71] because these are mild reaction conditions and commercially available bleach is used as oxidant.

Table 4.1. Catalytic epoxidation of styrene with bleach.[a]

Catalyst	Temperature (°C)	ee (%)	Yield (%)
Jacobsen catalyst	0	47.2	53.4
Mn(sal-L-phe)	25	___	Trace

[a] Reaction conditions: 0.01 M catalyst, 1.54 M bleach, 1 M styrene, CH_2Cl_2 solvent. Jacobsen catalyst: (S,S)-(+)-N,N'-bis (3,5-di-tert-butylsalicylidene)-1,2-cyclohexanediamino-manganese chloride.

The results in Table 4.1 showed our catalyst gives poor activity for the epoxidation of styrene. The catalyst we used is more hydrophilic than Jacobsen catalyst due to amino acids used to synthesize the ligand. Mn(sal-L-phe) has fairly good solubility in aqueous bleach solution which leads to less contact with the styrene and easy oxidative decomposition of the complex. We also repeated the Jacobsen epoxidation reaction. The results obtained are similar to those reported in the literature[71] including the ee value and the yield of styrene oxide.

Different solvents were screened in order to find suitable reaction conditions to carry out the epoxidation reaction. Tertiary butylhydroperoxide (TBHP), a common oxidant used in olefin epoxidations, was used in screening reactions.

Table 4.2. Epoxidation of styrene in different solvent with TBHP [a]

Catalyst(M)	Solvent	TBHP(M)	Styrene(M)	Time(hr)	Yield(%)
Mn(sal-L-his)(0.01M)	$CHCl_3$	2	1	1	8.4*
Mn(sal-L-try)(0.005M)	c-Hexanol	1	0.5	24	0
Mn(sal-L-try)(0.005M)	Dioxane	1	0.5	2	1.1
Mn(sal-L-try)(0.013M)	CH_3OH	2.5	1.25	3	1.3
Mn(sal-L-try)(0.0025M)	Acetone	5	1.25	24	2.7

[a] Reactions were run at 25°C except * which was run at 0°C

The results listed in Table 4.2 show that TBHP is not a good choice of oxidant for the epoxidation of alkenes by manganese-salicylidene amino acid catalysts. Not only is the yield of the epoxide relatively low, but it is also rather unselective. One typical experiment showed when 5.22 mmol styrene oxide was formed, 7.31 mmol benzaldehyde, 1.07 mmol phenylacetaldehyde, 5.64 mmol acetophenone as well as several other unidentified products were also observed. Finding a good oxidant which gives both good activity and good selectivity for the catalytic epoxidation reaction is our next goal.

The results listed in table 4.3 clearly showed using hydrogen peroxide as an oxidant and methanol as a solvent provided the best conditions for epoxidation reactions. There is a significant advantage in using methanol as a solvent. Both hydrogen peroxide and styrene can be dissolved in methanol and thus the reaction can run homogeneously. While using dioxygen as an oxidant is always the ultimate goal in epoxidation chemistry, no epoxide was detected in our reaction using dioxygen as an oxidant.

Table 4.3 Epoxidation of styrene with different oxidant.[a]

Catalyst (M)	Oxidant (M)	Styrene (M)	Time (hr)	Yield (%)
Mn(sal-L-try)(0.013)	TBHP (2.5)	1.25	3	1.3
Mn(sal-L-try)(0.005)	Urea H_2O_2 (1)	0.5	10	1
Mn(sal-L-try)(0.005)	$Na_2CO_3 1.5H_2O_2$ (1)	0.5	20	2.8
Mn(sal-L-try)(0.013)	H_2O_2 (1)	0.5	2	17.3*
Mn(sal-L-his)(0.007)	Air (50psi)	0.67	1.5	0

[a] Reactions were run at 25°C except * which was run at 0°C. Methanol was used as solvent.

A series of manganese-(S,S)-L-tryptophan (S,S = 3,5-Br- salicylaldehyde, 4,6-OCH$_3$ salicylaldehyde, 5-Br salicylaldehyde, 3-OH-salicylaldehyde, 4,6-OH-salicylaldehyde) complexes were synthesized and their catalytic activities were tested via epoxidation of styrene. None of the complexes with substituted salicylaldehyde showed better activity than the corresponding unsubstituted complex as the results listed in

Table 4.4 Both the electronic and steric effects may contribute to the differences in the reactivity of the catalysts

Table 4.4 Epoxidation of styrene with different manganese N-substituted salicylidene-L- tryptophan catalysts [a]

Catalyst	Epoxide (× 10^{-3} M)
Mn(sal-L-try)	61
Mn(5-Br-sal-L-try)	37
Mn(4,6-OCH_3-sal-L-try)	17
Mn(3,5-t-Bu- sal-L-try)	5.6
Mn(3,5-Br-sal-L-try)	0.6
Mn(3-OH-sal-L-try)	trace
Mn(4,6-OH-sal-L-try)	1.2

[a] Reaction conditions 3.1 x 10^{-4} mole catalyst, 2.5 x 10^{-2} mole styrene, 5 x 10^{-2} mole H_2O_2, 40 ml CH_3OH The reaction was run at 0°C

Asymmetric Epoxidation

Several asymmetric epoxidation experiments were performed with Mn(sal-L-try) and Mn(sal-L-his) complexes using hydrogen peroxide as oxidant and methanol as solvent. These experiment conditions were varied from run to run. These variables included amount of hydrogen peroxide, amount of styrene, reaction temperature, and reaction time These experiments and results are summarized in Table 4.5

Unfortunately all the reactions described in Table 4.5 provided low ee values. Jorgenson[81] reported 4-5% ee of styrene oxide can be reached by using manganese(II)-

salicylidene-L-phenylalanine as catalyst, which is similar to the result we obtained. The only difference between our reaction and Jorgensen's was the oxidant. Jorgensen used expensive iodosylbenzene while we are using much cheaper hydrogen peroxide. Although the yield of epoxide is lower when using hydrogen peroxide, the ee values are nearly the same. Running the reaction at lower temperature (-78°C) did not improve the ee value.

Table 4.5. Asymmetric epoxidation of styrene with manganese salicylidene L-amino acid catalysts

Cat (M)	H_2O_2 (M)	Styrene (M)	Time (hr)	Temp (°C)	Yield (%)	ee (%)
Mn(sal-L-try)(0.006)	1.25	0.63	1	0	15	4.2
Mn(sal-L-try)(0.025)	0.63	0.36	24	-78	32	3.4
Mo(sal-L-phe)(0.01)	0.67	0.33	8	0	27.7	2.3

It has been reported that manganese N-salicylidene amino acid complexes are dimeric structures.[82] The structure shows the coordination of manganese to the phenolic oxygen, the imine nitrogen, and the carboxylate oxygen, which bridges two metal centers. The dimer has C_2 symmetry, with the chiral centers situated two bond lengths away from the transition metal center. Chiral recognition between the substrate and the catalyst is expected to be effective due to the close proximity of the chiral centers to the active metal site. A lack of steric bulk around the metal center of Mo(sal-L-aa) catalyst may contribute to the low enantioselectivity. Several approaches to the metal-oxo are possible, as indicated by arrows A, B, and C shown in Figure 4.7. The consequence is a decrease in asymmetric induction and a drop in enantioselectivity. The only discrimination is shown by arrow D, in which the R-group hinders the approach of the substrate to the metal center

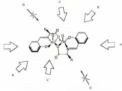

Figure 4 7 Various approaches to the metal center by the substrate

Introducing bulky groups onto the ligand may help increase enantioselectivity by reducing the number of pathways where substrates can approach the metal center This can be accomplished by using the more bulky 3,5 *tert*-butyl-salicylaldehyde for the synthesis of new ligands The results listed in Table 4 6 show that the ee value increased from ~3% to ~10% by using these new catalysts. The best result was obtained by adding base to the reaction system in order to neutralize free acid in the solution, which may protonate the carboxylate group in the complex and further decompose the catalyst.

Table 4.6. Asymmetric epoxidation of styrene with manganese 3,5-*tert*-butyl-salicylidene L-amino acid catalysts

Catalyst (M)	H_2O_2 (M)	Styrene (M)	Time (hr)	Temp (°C)	Yield (%)	ee (%)
Mn(*t*-Bu-sal-L-try) O_2 (0.006)	0.5	0.25	8	0	27.4	11.5*
Mn(*t*-Bu-sal-L-his) O_2 *t*-Bu-py 2KOH (0.125)	1	0.5	1	-78	19	15**

* H_2O_2 was added over three-hour period

** Reaction stopped in one hour

The relatively low ee value (< 20%) introduced by using substituted manganese salicylidene-L-amino acid complexes leads us to reconsider the model structure of our catalyst. When the oxidant approaches the catalyst, theoretically, it can form three metal-oxo isomers, which we think of as the active intermediates for enantioselective epoxidations. The structure in Figure 4.8a is expected to be most effective for inducing chiral recognition. The R-groups on the chiral center are *cis* to both oxo groups, and this configuration has the greatest influence on the orientation of incoming substrate molecules. The substrate must interact with the R group as it approaches the metal center and the favored orientation leads to asymmetric transfer of an oxygen atom. Oxygen transfer from both metal oxo groups to the substrate occurs in a chiral environment, and the highest possible enantioselectivity is achieved.

When the two oxo groups are *trans* to each other (Figure 4.8b), only one R-group is able to interact with the substrate. The environment around the metal center has a chiral influence for the R-group that is *cis* to the oxo group. This R-group interacts with the incoming substrate and the favored orientation leads to asymmetric transfer of oxygen atom. At the other metal center, the R group on the chiral center is *trans* to the oxo group and exhibits no substrate directing influences. Any substrate molecule that approaches this metal center will not be involved in asymmetric oxygen transfer.

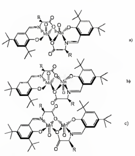

Figure 4.8 Possible orientations of the oxo group of the catalyst

No chiral recognition is expected for the isomer in which the oxo groups are *cis* to each other but *trans* to the R-groups (Figure 4.8c). Incoming substrate molecules do not interact with any R-groups since both R-groups are on the opposite side of the molecule from the oxo groups. Enantioselectivities are not expected with this isomer.

The inherent problem of the active species of each manganese salicylidene-L-amino acid catalyst forming isomers may account for the low enantioselectivity observed. If we assume an equal possibility of forming each metal oxo isomer the maximum ee value which can be reached is 50%. This range is also based on the maximum non-bonding interactions between catalyst and substrate.

The instability of the dimer structure in the solution may also contribute to the low enantioselectivity. In the monomer structure, the fourth equatorial position can be filled by water or by any donor molecule in solution. The dissociation of the dimer to the monomer of the manganese salicylidene L-amino acid catalyst will lead to more open non-chiral introducing positions which can be reached by substrate as shown in Figure 4.9.

Experimental results for enantioselective epoxidation of olefins by manganese-salicylidene-amino acid complexes have indicated that the structure of the catalyst may not be rigid enough to suppress the excess degree of freedom in the transition state which leads to lack of control the stereochemistry of the product. On the other hand the successful Sharpless catalyst, Jacobsen-Katsuki catalyst and chiral metalloporphyrin catalyst, which contain at least two chiral carbon atoms near the metal center, only one chiral center is introduced in our catalyst system. Both the flexible structure and the less chiral nature of the catalyst may account for the low ee value we obtained in our system.

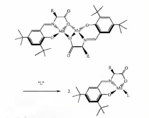

Figure 4.9 Dissociation of the dimer structure

Conclusions

A new type of manganese Schiff base complexes derived from optically pure amino acids was successfully synthesized and the use of these complexes as enantioselective epoxidation catalysts investigated

Screening various epoxidation reactions indicated using the environmental friendly oxidant hydrogen peroxide in methanol forms the most effective catalytic system for styrene epoxidation reactions

Enantioselective styrene epoxidations using unsubstituted manganese salicylidene L-amino acid complexes Mn(sal L-aa) introduces low ee values of around 3% Substituting bulky group onto the ligand helps increase enantioselectivity to 15% ee

Although enantioselectivities were below 20% ee, the novel use of manganese salicylidene-L-amino acid complexes as catalysts for enantioselective epoxidations shows promise by utilizing inexpensive raw materials to synthesize these catalytic compounds.

CHAPTER 5
OXIDATION OF MUSTARD SIMULANTS CATALYZED BY BICARBONATE SALTS

Introduction

The safety and environmental impact of the destruction of chemical warfare agents (CWA) are of great concern to the public.[83] In the United States, thousands of tons of chemical warfare agents such as mustard gas and Sarin are stockpiled at different storage sites.[84] The conventional way of destroying chemical warfare agents is by incineration. On the other hand, chemical neutralization is also being considered. At least two advantages are associated with chemical neutralization of chemical warfare agents. First, it is possible to convert chemical warfare agents to useful chemical compounds. Second, battlefield decontamination is also required in some specific cases, while incineration is not an option under such conditions.

Figure 5.1 listed some common chemical warfare agents. **HD,** also called as mustard gas, is a blistering agent that attacks the mucous membranes and is lethal at high doses.[85] **VX, GB** and **GD** are called "nerve" agents, which can stop respiratory and nervous functions and can kill people in minutes. The reaction chemistry of these agents is shared by a range of organic compounds such as sulfides, alkyl chlorides, organophosphorus esters, and pesticides.

Mustard (HD)

bis(2-chloroethyl)sulfide

Sarin (GB)

Propan-2-yl methylphosphono fluoridate

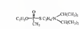

VX S-2-(Dipropan-2-ylamino)ethyl O-ethyl methylphosphonothioate

Tabun (GA) N,N-dimethyl-Phosphoramidocyanidate

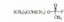

Soman (GD) 1,2,2,-trimethylpropyl methylphosphono-fluoridate

Lewisite (L) Dichloro[(E)-2-chloro ethyl] arsine

Figure 5.1. Structures of some common chemical warfare agents

A common decontaminant used is bleaching powder which basically contains hypochlorite salts The vigorous reactions of chemical agents with excess bleach are able to convert both neat and thickened agents to less or nontoxic products **HD** is converted into a series of oxidation and elimination products [86] **G** agents can also be rapidly detoxified in bleach solution. Since acid is produced in the process of detoxification of **G** agents, excess of hydroxide ion is required.[87] Bleach can be used for the decontamination of **VX**, particularly at low pH **VX** readily dissolves in acidic solutions via protonation of the nitrogen while the sulfur is oxidized rapidly by HClO. In alkaline bleach solution, the solubility of **VX** is significantly decreased. The deprotonated nitrogen is oxidized accompanied by the evolution of chlorine or oxygen gas and the formation of sulfate and carbonate salts. More than 10 moles of active chlorine are required to oxidize 1 mole of **VX** in alkaline solution.

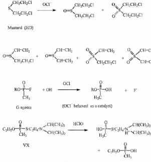

Figure 5.2 Decontamination of **HD**, G agents and **VX** by bleach.

There are some disadvantages for using hypochlorite as a decontaminant. Due to the instability of the bleach solution, fresh solution must be prepared prior to each use. Bleach is not a very efficient decontamination agent, excess amounts of bleach are required for the oxidation of chemical warfare agents. Bleach is corrosive to many surfaces and is ineffective in cold weather operation.

Another common decontaminant is called **DS2**. It is a general purpose, ready to use, reactive decontaminant with long-term storage stability and a wide operating temperature range (-26 to 52°C). This polar, non-aqueous liquid is composed, by weight, of 70% diethylenetriamine ($H_2NCH_2CH_2NHCH_2CH_2NH_2$), 28% ethylene glycol monomethyl ether ($CH_3OCH_2CH_2OH$) and 2% sodium hydroxide. The active component in **DS2** was found to be $CH_3OCH_2CH_2O^-$.[88] At ambient temperature, this base reacts with all four major chemical warfare agents (Figure 5.3). While **DS2** is a highly efficient decontaminant and is non-corrosive to most metal surfaces, it can damage paints as well as plastics, rubber, and leather materials. **DS2** is also corrosive to skin. Short contact-time and followed by a water rinse are required for the use of **DS2**.

There are some other reports on the decontamination of chemical warfare agents, which use biodegradation,[89] catalytic oxidation reaction with transition metal catalyst.[90]

In this chapter, the chemistry of a new CWA decontamination agent, which was first reported by Drago and Frank,[91] will be described. This system is based on the oxidant peroxymonocarbonate (HCO_4^-), which is formed by the reaction of hydrogen peroxide with bicarbonate ion (Equation 5.1).

$$HCO_3^- + H_2O_2 \rightleftharpoons HCO_4^- + H_2O \quad (5.1)$$

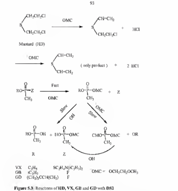

	R	Z
VX	C_2H_5	$SC_2H_4N(iC_3H_7)_2$
GB	iC_3H_7	F
GD	$(CH_3)_3CCH(CH_3)$	F

$^{-}OMC = OCH_2CH_2OCH_3$

Figure 5.3 Reactions of **HD, VX, GB** and **GD** with **DS2**

The existence of the peroxymonocarbonates has been reported for at least 70 years [92] Those indirect evidences have been derived either from analytical methods or from the preparative route and the ability to give off oxygen Firsova[93] and Jones[94] reported the synthesis of alkali metal peroxymonocarbonates ($MHCO_4$) Based on the evidence from vibrational spectra (IR, Raman), the structure of peroxymonocarbonate was suggested to contain a C O-O linkage, which is not present in the common adduct of alkali-metal carbonate with hydrogen peroxide (M_2CO_3 nH_2O_2). The presence of a peroxymonocarbonate species in solution has also been inferred from Raman and ^{13}C NMR spectroscopy. Similar evidence was also presented for the presence of CO_4^{2-} in solutions prepared by dissolving solid peroxymonocarbonate in aqueous solution.[95] The crystal structure of a peroxomonocarbonate, $KH(O_2)CO_2 \cdot H_2O_2$, was determined last year (Figure 5.4).[96]

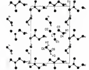

Figure 5.4: Section of the crystal structure of $KH(O_2)CO_2 \cdot H_2O_2$ along [010].

The previous oxidation system developed by Drago and Frank has shown excellent catalytic oxidation of ethylphenyl sulfide to ethyphenyl sulfoxide and ethylphenyl sulfone by formation of strong oxidant peroxymonocarbonate.[91] However, the limited solubility of $NaHCO_3$ in H_2O / *t*-BuOH mixed solvent has restricted the further enhancement of the catalytic ability of the novel oxidation system. Our work has focused on searching a bicarbonate or carbonate salt that has good solubility in alcohol-water mixed solvent and excellent reactivity for oxidation reactions.

Experimental

Reagents and Equipment

Unless otherwise stated, all reagents were obtained from commercial sources and used without further purification. Gas chromatographic analyses on volatile products and reactants were carried out by using a Hewlett Packard model 5890 gas chromatograph equipped with Hewlett Packard 50+ column (crosslinked 50% phenyl methyl – 30 m × 0 53 mm × 1.0 μm film thickness) and helium as the carrier gas, a flame ionization detector and a Hewlett Packard 3396 Series II integrator Substrates and products were identified via comparisons with known standards Calibration curves were used to relate peak areas to the number of moles of products and reactants.

Preparation of $(CH_3)_2CHCH_2NH_3HCO_3$

This compound is prepared simply by bubbling CO_2 gas into $(CH_3)_2CHCH_2NH_2$ solution in ice bath. White precipitate was formed and stored in a refrigerator

General Procedure for the Oxidation of Ethylphenyl Sulfide

The appropriate amounts of catalyst were added to an organic/water mixed solution containing ethylphenyl sulfide Hydrogen peroxide was added to the reaction and reactions were run at 25 °C Reactant consumption and reaction products were monitored and quantified by GC The moles of each of the reactants and the known products were determined using calibration curves for each compound

Results and Discussion

Variation of Carbonate and Bicarbonate Salts

We screened several different salts by testing the reactivity of oxidation of ethylphenyl sulfide. The results are listed in Table 5.1.

Table 5.1 Oxidation of ethylphenyl sulfide catalyzed by different salts.[a]

Salt	$t_{1/2}$ (min.)
$NaHCO_3$	70
$KHCO_3$	75
NH_4HCO_3	55
Na_2CO_3	433
$(CH_3CH_2CH_2)_4NHCO_3$[b]	177
NH_4HCO_3 (10^{-4}mol H_3O^+)	45
Blank	133

[a] Reaction conditions: 7.5 mL *t*-butanol, 3 mL H_2O, 4.8 × 10^{-4} mol salt (0.035M), 2 mL 35% H_2O_2 (1.7 M), 8.2 × 10^{-3} mol ethylphenyl sulfide(0.6 M), 0.2 mL chlorobenzene as internal standard. The reactions were run at 25°C and were followed by GC. The experimental error for the determination of the half-life ($t_{1/2}$) of the reaction is ± 5 minutes.

[b] Salt generated *in situ*

The reaction rates are greatly influenced by the nature of the salts employed. Better reactivity can be achieved by using NH_4HCO_3 rather than $NaHCO_3$, which was used in our previous study. The catalytic reaction is apparently quenched by using Na_2CO_3. This result may indicate that the reaction is pH dependent. Adding small amounts of acid to the system slightly increased rate of the reaction, suggesting that lower pH favors the oxidation reaction. We decreased the concentration of H_2O_2 from 4.2 M to 1.7 M in our reaction system in order to increase the reaction efficiency and get accurate experimental results.

There is an advantage in using NH_4HCO_3 to replace $NaHCO_3$. The higher solubility of NH_4HCO_3 in alcohol-water mixed solvents allows us to put more catalyst in the solution to facilitate the reaction. The reaction rate increased dramatically by adding 5 times more catalyst (NH_4HCO_3). The results are summarized in Table 5.2.

Table 5.2. Oxidation of ethylphenyl sulfide catalyzed by different amount of NH_4HCO_3 [a]

NH_4HCO_3 (M)	$t_{1/2}$ (min)
0.035	55
0.105	12
0.175	7

[a] Reaction conditions: 7.5 mL *t*-butanol, 3 mL H_2O, 2 mL 35% H_2O_2 (1.7 M), 8.2×10^{-3} mol ethylphenyl sulfide(0.6 M), 0.2 mL chlorobenzene as internal standard. The reactions were run at 25°C and were followed by GC. The experimental error for the determination of the half-life ($t_{1/2}$) of the reaction is ± 5 minutes.

Influence on the Amount of Water

The preliminary mechanistic study proposes that the reaction first reach the equilibrium for the formation of active peroxymonocarbonate anion followed by oxygen transfer from peroxymonocarbonate to substrate (Equation 5.1). The equilibrium will shift to the right side by reducing the amount of water presenting in the system. Theoretically, the oxidation reaction will speed up by the formation of more active peroxymonocarbonate intermediate.

Table 5.3 Influence on the amount of water[a]

H_2O (M)	$t_{1/2}$ (min)
21.6	58
17.5	20
13.4	20
9.4	30
5.3	>90

[a] Reaction conditions 2 mL 35% H_2O_2 (1.7 M) 4.1×10^{-3} mol ethylphenyl sulfide (0.3 M), 4.8×10^{-4} mol NH_4HCO_3 (0.035 M) 0.2 mL chlorobenzene as internal standard. The volume of the solution is keeping constant as $V_{t\text{-butanol}} + V_{water} = 10.5$ (mL). The reactions were run at 25°C and were followed by GC. The experimental error for the determination of the half life ($t_{1/2}$) of the reaction is ± 5 minutes

Table 5.3 lists the experimental results obtained when the concentration of water in the system is varied. The results are not what we expected. At the beginning, cutting the amount of water in the system increased the reactivity as we expected. But, when the concentration of water in the system is too low, the decreasing of the polarity of the system and lower solubility of bicarbonate catalyst may become the predominant factor to slow down the reaction.

Oxidation of Ethylphenyl Sulfide in Different Solvents

Water- *t*-butanol mixed solvent is used in our reaction system to give good solubility to both organic sulfide and inorganic bicarbonate salts. *t*-Butanol is a good choice, because it is non toxic, cheap, stable, and can be mixed with water; however, the high melting point (25°C) of *t*-butanol limits the use of this solvent especially in cold weather. We have screened several organic solvents as substitutes for *t*-butanol

(Table 5.4). Ethanol is the best solvent we found. No oxidation products of ethanol were found in the reaction system.

Table 5.4. Solvent variation.[a]

Solvent	$t_{1/2}$ (min)
t-butanol	55
$CH_3C(O)CH_3$	360
CH_3OH	120
C_2H_5OH	40
C_2H_5OH (CO_2 saturated)	40
$(CH_3)_2CHOH$	52
$HOCH_2CH_2OH$	120
p-Dioxane	160
C_2H_5OH (blank)	110

[a] Reaction conditions: 7.5 mL solvent, 3 ml H_2O, 2 mL 35% H_2O_2 (1.7M), 8.2 × 10^{-3} mol ethylphenyl sulfide(0.6M), 4.8 × 10^{-4} mol NH_4HCO_3 (0.035M), 0.2 mL chlorobenzene as internal standard. The reactions were run at 25°C and were followed by GC. The experimental error for the determination of the half-life ($t_{1/2}$) of the reaction is ± 5 minutes.

Synthesis and Reactivity of $(CH_3)_2CHCH_2NH_3HCO_3$

Bicarbonate salts with a large organic counter-ion have good solubility in alcohol-water mixed solvents. The excellent results by using large amount of NH_4HCO_3 listed in Table 5.2 prompted us to further increase the size of the counter-ion of bicarbonate salt in an attempt to improve solubility of the catalyst.

$(CH_3)_2CHCH_2NH_3HCO_3$ is easily to prepare simply by bubbling CO_2 gas into $(CH_3)_2CHCH_2NH_2$ solution as shown in Equation 5.2. White precipitation forms immediately.

$$H_2O + CO_2 + (CH_3)_2CHCH_2NH_2 \rightleftharpoons (CH_3)_2CHCH_2NH_3HCO_3 \quad (5.2)$$

The isolated compound was used to test the solubility and reactivity for the oxidation of ethylphenyl sulfide The results were also compared to NH_4HCO_3 as catalyst (Table 5 5)

Table 5.5. Influence on the Size of Counter-Cation.[a]

Salt (M)	$t_{1/2}$ (min.)
$(CH_3)_2CHCH_2NH_3HCO_3$ (0.35 M)	17
NH_4HCO_3 (0 035 M)	55
NH_4HCO_3 (0 105 M)	12

[a] Reaction conditions. 7 5 mL *t*-butanol 3 mL H_2O, 2 ml 35% H_2O_2 (1 7 M). 8.2×10^{-3} mol ethylphenyl sulfide(0 6 M), 0 2 ml chlorobenzene as internal standard. The reactions were run at 25°C and were followed by GC The experimental error for the determination of the half-life ($t_{1/2}$) of the reaction is ± 5 minutes.

$(CH_3)_2CHCH_2NH_3HCO_3$ is not as active as NH_4HCO_3 at same concentration but has a much better solubility We have not reached the saturation of the solution by adding 10 times more $(CH_3)_2CHCH_2NH_3HCO_3$ salts in to the solution The results are promising for increasing the reaction rate by adding large amount of bicarbonate salt

Conclusions

The monocarbonate decontamination system has been improved by alteration of solvent and count ion in bicarbonate By using NH_4HCO_4 as catalyst and C_2H_5OH/H_2O

as solvent, the reaction rate for the oxidation of mustard simulant, ethyl phenyl sulfide (EtPhS), can be increased 10 times compared with the original system using $NaHCO_3$ as catalyst and *t*-$BuOH/H_2O$ as solvent. The synthesis of a new bicarbonate salt with a large organic cation, $(CH_3)_2CHCH_2NH_3HCO_3$, makes it possible for the further increasing the reaction rate by adding more to the reaction system

CHAPTER 6
ACTIVATION OF HYDROGEN PEROXIDE IN BASIC AQUEOUS SOLUTION BY COPPER (II) WITH 2-PYRIDYLACETIC ACID

Introduction

Catalytic oxidation reactions in aqueous media have received much attention recently.[97] Water is an ideal solvent to carry out oxidation reactions from both a practical as well as environmental standpoint.

Water-soluble manganese porphyrin complexes are very good catalysts for doing oxidation reactions in aqueous media. Zheng and Richardson used a water soluble manganese porphyrin catalyst to oxidize different organic substrates using Oxone or magnesium monoperoxyphthalate (MMPP) as oxidants.[98] Olefins can be oxidized to epoxides or the corresponding hydrolyzed diol products. Alcohols can be oxidized to ketones and aldehydes can be oxidized to acids. There are some other examples of metal porphyrin catalyzed oxidation of organic substrates. Song synthesized Vitamin K_3 and 6-methyl-1, 4-naphthoquinone by metalloporphyrin-catalyzed oxidation of 2-methylnaphthalene using potassium monopersulfate as oxidant.[99] Hodges reported the oxidation of azo dyes by sterically hindered anionic oxoiron (IV) porphyrin in aqueous solution.[100] There is considerable interest in dye oxidation reactions because of the need to be able to oxidize dyes in industrial effluent[101] and maintain the color of dyed fabrics during washing processes[102] or through photo-oxidation in sunlight.[103] Kinetic investigations were done for the oxidation of substituted arylazonaphthol dyes by hydrogen peroxide in alkaline solution[104] and oxidation of Methyl Orange and substituted arylazonaphthol dyes.[105]

It is a surprising that unactivated C-H bonds can be oxidized in aqueous media catalyzed by platinum catalysts. For example, aliphatic carboxylic acids can be converted to the corresponding hydroxycarboxylic acid. The order of preference for the oxidation of C-H bonds in aliphatic carboxylic acids are α-C-H <<β-C-H < γ-C-H ≥ δ-C-H ≈ ε-CH.[106] Ethers, alcohols, esters, and light alkanes were also oxidized by platinum catalysts.[107]

Rabion studied the biomimetic oxidation in water with water-soluble alcohols as substrates. Water-stable iron catalysts were used, which mimic methane monooxygenase enzyme (MMO).[108]

Some manganese 1,4,7-triazacyclononane complexes have been shown to be effective catalysts for the oxidation of a variety of organic substrates with H_2O_2.[109] In this system, an oxo-manganese (V) species has been identified by using electrospray mass spectrometry for the reaction of manganese triazacyclononane complexes with H_2O_2 and 4-methoxyphenol in aqueous solution.[110]

A large number of patents address the goal of replacing commercial hypochlorite-containing bleaches.[111] An earlier report from this laboratory describes the study of several copper complexes that activate hydrogen peroxide for catalytic oxidation in basic solution.[97c] Bidentate ligands were shown to produce the most effective copper (II) complexes for the oxidation of quinaldine blue(pinacyanol chloride) in basic aqueous solution. The oxidation was proposed to proceed through a dissociative mechanism for coordination of hydroperoxide to the copper (II) center leading to a rate law in the form of the Michaelis-Menton equation. The experimental rate law is that expected for nucleophilic attack on the coordinated hydroperoxide resulting in oxygen atom transfer [16]

We report here the synthesis, characterization and reactivity of a series of different complexes of 2-pyridylacetic acid that form at different ligand to copper (II) ratios. A novel complex composition in the series is characterized by single crystal X-ray diffraction. The activity of these complexes as catalysts for activation of hydrogen peroxide is investigated by measuring the rates of oxidation of quinaldine blue. Rates up to an order of magnitude faster than the related copper (II) catalyst systems previously reported are observed. Furthermore, these systems are able to oxidize a wider variety of substrates than the earlier complexes.

Experimental

Materials and Physical Measurements.

All of the starting materials are commercially available and were used as received. UV-visible measurements were performed on a Perkin-Elmer Lambda-6 spectrophotometer at room temperature. All pH measurements were made with a calibrated Fisher Accumet model 630 pH meter.

Preparation of $Cu_2(PYAA)Cl_3 \cdot 0.5H_2O$

An aqueous solution of 2-pyridylacetic acid hydrochloride (2.5 mmol) was neutralized with KOH. A $CuCl_2$ aqueous solution (5 mmol) was added dropwise. The solution was stirred at 90°C overnight, and a green precipitate resulted. After filtration, the powder was washed with methanol and dried under vacuum (yield 85%). Anal. Calcd for $Cu_4C_{14}H_{14}N_2O_5Cl_6$: C, 22.21, H, 1.86; N, 3.70. Found: C, 22.61; H, 2.00; N, 3.96

Preparation of Cu(PYAA)Cl

A methanol solution (10mL) of 2-pyridylacetic acid hydrochloride (0.45 M) was neutralized with triethylamine (9 mmol). A methanol solution (10 mL) of $CuCl_2$ (0.45 M) was added dropwise. The blue precipitate was filtered, washed with methanol and dried under vacuum (yield 90%). Anal. Calcd for $Cu_1C_7H_6N_1O_2Cl_1$: C, 35.76, H, 2.57, N, 5.96. Found: C, 36.09; H, 2.90; N, 6.01

Preparation of Cu(PYAA)$_2$·0.5H_2O

An aqueous solution (10 mL) of 2-pyridylacetic acid hydrochloride (0.5 M) was neutralized with KOH (5 mmol). 10 mL $CuCl_2$ solution (0.25 M) was added dropwise at room temperature. A purple precipitate was formed washed with water and dried under vacuum (yield 93%). Anal. Calcd for $Cu_2C_{28}H_{26}N_4O_9$: C, 48.77, H, 3.80, N, 8.12. Found: C, 48.84; H, 4.00, N, 8.08

Preparation of $Cu_2C_{28}H_{28}N_4O_8$·4.5H_2O

An aqueous solution (10 mL) of 2-pyridylacetic acid hydrochloride (0.5 M) was neutralized with KOH (5 mmol). 10mL copper (II) chloride solution (0.25 M) was added dropwise, and a blue precipitate was formed. The solution was heated to 90°C and the precipitate dissolved. KOH (0.05 M) was added to increase the pH to 8.0. After standing the solution for 48 hours, dark blue crystals were formed. The crystals were harvested, washed with water, and dried under vacuum (yield 67%). Anal. Calcd for $Cu_2C_{28}H_{26}N_4O_9$: C, 48.77, H, 3.80; N, 8.12. Found: C, 48.84, H, 4.00, N, 8.08. The crystals for the structure determination were grown from a methanol/dichloromethane mixture

X-ray Structure Determination of $Cu_2C_{28}H_{20}N_4O_6 \cdot 4.5H_2O$

X-ray crystallography work was done by Dr K. A. Abboud at the Department of Chemistry, University of Florida Data were collected at room temperature on a Siemens R3m/V diffractometer equipped with a graphite monochromator using MoKa radiation ($\lambda = 0.71073$ Å) 40 reflections with $20.0° < 2\theta < 22.0°$ were used to refine the cell parameters 3482 reflections were collected using the ω-scan method. Four reflections were measured every 96 reflections to monitor instrument and crystal stability (maximum correction on I was < 2.00 %)

The structure of $Cu_2C_{28}H_{20}N_4O_6 \cdot 4.5H_2O$ was solved by the Direct Methods in SHELXL-97, and refined using full-matrix least squares [11] The non-H atoms were treated anisotropically, whereas the hydrogen atoms were calculated in ideal positions and were riding on their respective carbon atoms The asymmetric unit consists of a half complex, two water molecules in general positions and one water molecule (O_5) on a 222 symmetry element. The water H atom were located from a difference Fourier map and were riding on their parent O atoms with displacement parameters equal to 1.2 of the parent O atoms. One H atom was located on the O_5 water and its occupation factor was fixed at 0.5 because of symmetry A total of 193 parameters were refined in the final cycle of refinement using 1990 reflections with $I > 2s(I)$ to yield R_1 and wR_2 of 4.44% and 8.72%, respectively. Refinement was done using F_2 The abbreviated crystallographic data for $Cu_2C_{28}H_{20}N_4O_6 \cdot 4.5H_2O$ is listed in Table 6.1

Table 6.1. Crystal data and structure refinement for $Cu_2C_{26}H_{20}N_4O_6 \cdot 4.5H_2O$

Empirical formula	$C_{26}H_{20}Cu_2N_4O_{10.50}$
Formula weight	692.61
Temperature	293(2) K
Wavelength	0.71073 Å
Crystal system	Orthorhombic
Space group	Fddd
Unit cell dimensions	a = 19.568(4) Å, b = 22.476(5) Å, c = 25.573(5) Å. α = 90° β = 90° γ = 90°
	Volume = 11247(4) $Å^3$ Z = 16
Density (calculated)	1.636 Mg/m^3
Absorption coefficient	1.579 mm^{-1}
F(000)	5680
Crystal size	0.32 × 0.21 × 0.15 mm
Theta range for data collection	1.59 to 27.50°
Limiting indices	$0 \le h \le 25$, $0 \le k \le 29$, $0 \le l \le 33$
Reflections collected	3482
Independent reflections	3235 [R(int) = 0.0000]
Absorption correction	None
Refinement method	Full-matrix least-squares on F^2
Data / restraints / parameters	3235 / 0 / 193
Goodness-of-fit on F^2	1.029
Final R indices [I>2sigma(I)]	R_1 = 0.0444, wR2 = 0.0872 [1990]
R indices (all data)	R_1 = 0.0854, wR2 = 0.0946
Largest diff. peak and hole	0.480 and 0.451 e.$Å^{-3}$

Results and Discussion

Oxidation of Quinaldine Blue by Copper (II) Chloride with 2-Pyridylacetic Acid at Different Ligand : Metal Ratios

Catalysts for the activation of hydrogen peroxide were screened by forming complexes in solution from stock solutions of copper (II) chloride and 2-pyridylacetic acid. Activity was measured by following the rate of oxidation of a redox indicator, quinaldine blue. The ratio of 2-pyridylacetic acid to copper chloride in the catalyst solution was varied in a series of oxidation reactions in which the metal concentration was kept constant. The influence of the ligand : metal ratio on the rate of oxidation of quinaldine blue by hydrogen peroxide is given in Table 6.2.

Table 6.2 Rate of quinaldine blue oxidation with varying ratios of 2-pyridylacetic acid to $CuCl_2$ [a]

Ligand : Metal Ratio	Rate of Oxidation (M / s)
1:1	0.25×10^{-7}
2:1	0.44×10^{-7}
4:1	1.12×10^{-7}
8:1	2.85×10^{-7}
12:1	2.28×10^{-7}
24:1	0.76×10^{-7}

[a] [Copper (II)] = 2.9×10^{-5} M, [H_2O_2] = 2.9×10^{-4} M, [quinaldine blue] = 3.0×10^{-5} M. All reaction solutions were buffered at pH 9.1 using a borate buffer. Rate measured by UV-visible spectrophotometer at λ_{max} = 600 nm, monitoring the decrease in quinaldine blue concentration vs. time. Rate of oxidation was determined through the method of initial rates and corrected for the background reaction in the absence of catalyst.

The most active catalytic system is obtained at an 8:1 ligand : Cu (II) ratio. With the Cu (II) complexes studied earlier,[27c] ligand : metal ratios of 1:1 produced the most active oxidation catalysts and excess ligand slowed the rate of oxidation.

A spectroscopic investigation was done in an attempt to determine why a high ratio of ligand : metal is beneficial for the 2-pyridylacetic acid system. The UV-visible spectrum at a fixed concentration of Cu (II) gives no new bands as ligand is added above a 2:1 ligand : metal ratio but showed a continuous increase in absorbency as the ligand was added up to an 8:1 ligand : metal ratio.

We attempted to use Job's method to determine the composition of copper (II) complex with 2-pyridylacetic acid in the solution. Job's method [112] employs spectra of a series of solutions of widely varying mole ratios of ligand to metal, with the same total number of moles of ligand plus metal, to determine the composition of complexes formed in a solution. There is a limitation using Job's method to determine the composition of a metal complex. Some trouble may be encountered in dealing with a weak complex, for the absorbance curve will be quite flat in the vicinity of the maximum.[112] The results of Job's experiments for the 2-pyridylacetic acid /Cu (II) system gave flat absorbance curves, and the position for the maximum absorbency is dependent on the wavelengths chosen for the analysis. It is not appropriate for using Job's method to determine the composition for the 2-pyridylacetic acid / Cu (II) system. The results from Job's method experiments also indicate that there is no predominate species in the solution for the 2-pyridylacetic acid / Cu (II) system. Several copper (II) complexes with different ligand : metal ratio may exist simultaneously in the solution.

The oxidation products of quinaldine blue were not determined in this study. Byers[113] oxidized quinaldine blue by a photooxidation method and a 30% yield of N-ethyl-2-quinolone was isolated as oxidation product. Some of the initial oxidation products are labile and degrade further.

Isolation and Characterization of Solid Complexes

The promising catalytic results encouraged the synthesis of complexes of 2-pyridylacetic acid and copper (II). The synthesis of $Cu(PYAA)_2$ complex has been reported by other workers and the crystal structure has been determined.[114] In $Cu(PYAA)_2$, a six coordinate Cu (II) is surrounded by an octahedral arrangement of two pyridine nitrogen atoms and two carboxyl oxygen atoms belonging to the same chelate molecule, and of two other carboxyl oxygen atoms at the vertices, belonging respectively to the lower and upper molecules. No any other characterization of 1:2 and 1:1 ligand to metal ratio compounds are found in the literature. We successfully isolated $Cu_2(PYAA)Cl_3 \cdot 0.5H_2O$ and $Cu(PYAA)Cl$ complexes, which may exist in the solution.

An interesting complex was also isolated from a 2:1 solution of 2 pyridylacetic acid and copper (II) that was heated to 90°C to drive off water. Elemental analyses results indicated that $Cu(PYAA)_2$ was not obtained. The crystal structure of the complex has been determined by X-ray crystallography. An ORTEP view of the complex is shown in Figure 6.1. In this complex, the ligand (PYAA) has undergone oxidative degradation. One of the 2-pyridylacetic acid ligands lose CO_2 and condense with another 2-pyridylacetic acid to give a tetradentate ligand: 2-py-CO-CH(CO_2H)-2-py. This results in a copper (II) dimer with an unusually short Cu-Cu distance (2.9 Å). Each Cu(II) is five coordinated with distorted square pyramidal geometry. All the bond lengths are in the normal bond length range except the longer Cu-O3 bond (2.23 Å) which indicates weaker interaction because of rigid complex configuration

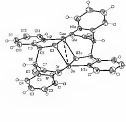

Figure 6.1. Crystal structure of $Cu_2C_{26}H_{20}N_4O_8 \cdot 4\ 5H_2O$

Metal assisted ligand oxidation is reported in the literature 2,2' Bipyridine was first prepared in more than one hundred years ago from the distillation of a basic aqueous solution of the transition metal complexes of 2 pyridinecarboxylate [115] Two recent published papers also discussed about this issue [116]

The isolated complexes were used for the oxidation of quinaldine blue In all instances except for the complex in Figure 6 1, the complex behaved the same as the comparable ratios of ligand to Cu (II) Addition of excess ligand to the solution containing isolated complexes increased reactivity for the oxidation reaction The complex in Figure 6 1 was not as active as the other isolated complexes in part because of its lower solubility in water

We do not know the complexes responsible for the most efficient catalysis. Our earlier results[16] with copper (II) complexes suggest that the 1 1 Cu (II)/PYAA complex should be the most active species in solution and Cu(PYAA)$_2$ should be less active One possible explanation is that the high ligand : metal ratio is needed to avoid the hydrolysis of copper(II) species in basic solution, which will decompose the catalyst So an 8 1 ratio may maximize the concentration of the active catalyst which we shall refer to as CuPYAA As the ratio of ligand to metal increases above an 8 1 ratio, the CuPYAA complex is converted to the Cu(PYAA)$_2$ complex which leads to decrease the catalytic activity Similar results were reported by Barton[117] for the oxidation of hydrocarbons by using Fe^{II}-picolinic acid as a catalyst A system with Fe^{III} / picolinic acid = 1 4 was optimum for oxidation of saturated hydrocarbons, while using 10 equivalents of picolinic acid actually slightly decreased the oxidation reaction rate

Effect of Complex and Peroxide Concentration on the Reaction Rate

The oxidation of quinaldine blue was performed with differing amounts of copper (II) and hydrogen peroxide keeping the ratio of ligand to metal at 4 1 in all the experiments The results show that the reaction is also first order in copper (II) complex (Figure 6 2) This is in agreement with the results of our earlier work on peroxide activation with copper (II) complexes [97c] A Lineweaver-Burk plot of $1/[HO_2^-]$ vs 1/(rate) (Figure 6.3) gives a straight line, indicating that the reaction follows Michaelis-Menton kinetics (Figure 6.4) consistent with the mechanism reported earlier for activation of peroxide by copper (II) complexes of other bidentate ligands.

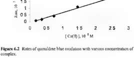

Figure 6.2 Rates of quinaldine blue oxidation with various concentration of copper (II) complex.

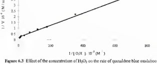

Figure 6.3 Effect of the concentration of H_2O_2 on the rate of quinaldine blue oxidation

$$H_2O_2 \xrightleftharpoons{K_a} O_2H^- + H^+ \qquad K_a = 1.78 \times 10^{-12}$$

$$LCu^{II}(H_2O)_4 \underset{k_{-1}}{\overset{k_1}{\rightleftharpoons}} LCu^{II}(H_2O)_3 + H_2O$$

$$Cu^{II}(H_2O)_3 + O_2H^- \xrightarrow{k_2} LCu^{II}(H_2O)_2(O_2H^-)$$

$$LCu^{II}(H_2O)_2(O_2H^-) + \text{substrate} \xrightarrow{\text{Fast}} \text{Product} + LCu^{II}(H_2O)_4$$

$$\text{Rate} = k_2\,[LCu^{II}(H_2O)_3]\,[O_2H^-]$$

$$= \frac{k_1 k_2\,[LCu^{II}(H_2O)_3]\,[O_2H^-]}{k_{-1} + k_2\,[O_2H^-]}$$

$$\text{Rate} = \frac{V_{max}\,[O_2H^-]}{K_m + [O_2H^-]}$$

$$V_{max} = k_1[LCu^{II}(H_2O)_4] \qquad K_m = k_{-1}/k_2$$

Figure 6.4: Kinetics for oxidation reaction catalyzed by copper (II) complexes

The rates of reaction for oxidation by CuPYAA are considerably faster than for complexes reported earlier. Since all the copper complexes studied followed Michaelis-Menton kinetics, they can be compared based on the V_{max} values obtained from plots of

$1/[HO_2^-]$ vs. 1/rate. The V_{max} for the Cu/ PYAA system is 5.1×10^{-5} M s^{-1} for a copper complex concentration of 2.8×10^{-5} M. This is much higher than that for the Cu/picolinic acid system, where the V_{max} was only 7.9×10^{-7} M s^{-1}[97c] The V_{max} values show that CuPYAA is a better catalyst for activation of peroxide in basic solution than any of the copper(II) complexes studied earlier.

Oxidation of Other Substrates by CuPYAA

CuPYAA-catalyzed oxidation of different alcohols by hydrogen peroxide were examined at the same conditions used in the quinaldine blue oxidation. Table 6.3 shows the percentage conversion to oxidized products for different ligand and metal ratios.

Table 6.3. Percentage conversion to oxidized products for varying ligand to metal ratios

Catalyst System	Allyl Alcohol % Conversion
$CuCl_2$ + 2PYAA	18
$CuCl_2$ + 4PYAA	32
$CuCl_2$ + 6PYAA	35
$CuCl_2$ + 8PYAA	33

[a] [Copper(II)] = 3×10^{-4} M, $[H_2O_2]$ = 3 M; [Allyl alcohol] = 3.0×10^{-4} M. All reaction solutions were buffered at pH 8.0 using a bicarbonate buffer. Percentage conversion was measured by gas chromatography after 24 hours.

In Table 6.3, we can find the similar trend obtained in oxidation of quinaldine blue. The conversion of oxidized products increases as we increase the ligand to metal ratio. However, the highest conversion for oxidizing allyl alcohol was around ligand to metal ratio around 6:1 which is not exactly the same as what we got at 8:1. Hydrogen peroxide is not very stable in the basic aqueous solution with metal catalyst.

Decomposition of hydrogen peroxide over long reaction periods may contribute to the lower conversion than we expected at high ligand to metal ratio.

Table 6.4 summarizes the results of oxidation of alcohol catalyzed by CuPYAA system. Different alcohols can be oxidized at room temperature in basic solution. The steric effect and the electric nature of the substrate have great influence on the rate of oxidation reaction.

Table 6.4. Oxidation of alcohol catalyzed by CuPYAA [a]

Substrate	Conversion(%)
Ethanol	9.4
1 Propanol	4.5
2 Propanol	16
Allyl Alcohol	5.3
2-Hexanol	10
Cyclohexanol	1

[a] [Copper(II)] = 6 × 10^{-4} M, [PYAA] = 2.4 × 10^{-3} M, [H_2O_2] = 0.7 M, [Alcohol] = 0.06 M. All reaction solutions were buffered at pH 8.0 using a bicarbonate buffer. Percentage conversion was measured by gas chromatography after 1 hours. There are no oxidation reactions in the absence of copper(II) catalyst.

Conclusions

In basic aqueous solution, copper (II) chloride and 2-pyridylacetic acid form a complex that is unusually active for the oxidation of organic substrates using hydrogen peroxide. The maximum concentration of the active species seems to occur when the ratio of ligand to metal is 8:1. At ratios above 8:1, significant concentrations of the copper complex with a weakly coordinated water are not present Several copper (II) complexes can be isolated from solutions containing copper (II) and 2-Pyridylacetic acid. The most interesting of these results form the condensation of two 2-Pyridylacetic acid ligands The crystal structure for this complex shows a copper (II) dimer with an unusually short Cu-Cu distance The isolated complexes require excess ligand for full catalytic efficiency, as addition of excess ligand to solutions made from the isolated complexes increases activity

REFERENCES

1 Hassall, C H *Org React* **1957,** *9,* 73

2 Lyons, J E. *Hydrocarbon Proc* **1980** 107

3 Davy, E *Philos. Trans R. Soc. London* **1820,** 108

4 Smidt, J , Hafner, W , Jira, R , Sedlmeier J , Sieber R , Ruttinger, R., Kojer, H *Angew Chem* **1959,** *71(5)* 176

5 Bedell K. A., Rainbird, H A *Hydrocarbon Proc* **1972,** *11* 141

6 Waddams A. L. *Chemicals from petroleum* 4th ed., London John Murray 1978

7 March J *Advanced organic chemistry* 4th ed New York Wiley **1992,** 1176

8 Heinemann, H in *Catalysis Science and technology* Vol 1 (J R. Anderson and M Boudart, eds) New York Springer-Verlag **1981,** 1

9 Martell, A E Sawyer, D T *Oxygen complexes and oxygen activation by transition metals* New York. Plenum Press **1988,** 35

10 Hock, H , Lang, B *Chem. Ber* **1944,** *77* 257

11 Drago R. S *Coord Chem. Rev* **1992,** *117* 185

12 James, B R. in *Catalysis of organic reactions* (W E. Pascoe ed.) New York Marcel Dekker **1992,** 246

13 Abeles, R. H , Frey, P A , Jencks, W P *Biochemistry* Boston Jones and Bartlett. **1992,** 87

14 Hamilton, G A. *J Am Chem. Soc* **1964,** *86* 3390

15 Smith, J G *Synthesis* **1984,** 629

16 Bartlett, P D *Rec Chem. Prog* **1957,** *18* 111

17 Drago R. S , Mateus, A. L. M. L., Patton, D *J Org Chem.* **1996,** *61* 5693.

18 Sheldon, R. A. *Top. Curr Chem.* **1993,** *164* 21

19 Bielanski A , Haber, J *Oxygen in catalysis* New York: Marcel Dekker **1991,** 456

20 Sheldon, R. A *J Mol Catal.* **1980,** *7* 107

21 Shilov, A E , Shul'pin, G A *Chem. Rev* **1997,** *97* 2879

22 Kohan, M I *Nylon plastics* New York: John Wiley **1973,** 14

23 Seymour, R B , Carraher, C E. Jr *Polymer chemistry* 2nd ed., New York Marcel Dekker. **1988,** 251.

24 Castellan, A , Bart, J. C J , Cavallaro, S *Catal Today* **1991,** *9* 237

25 Seymour R B Carraher C. E Jr *Polymer chemistry* 2nd ed , New York Marcel Dekker **1988,** 496

26 *Chem Eng News* **1990,** *68* 4

27 Thiemens, M. H , Trogler W C *Science* **1991,** *251* 932

28 (a) Du Pont *U S Patent* **1940,** 2,223,494 (b) Steeman J W M Kaarsemaker S Hoftyzer P *J Chem Eng Sci.* **1961,** *14* 139 (c) Miller S A , *Chem Process Eng (London)* **1969,** *50* 63 (d) Tanaka K. *Chem. Tech.* **1974,** 555 (e) Schuchardt, U Pereira, R. Rufo, M *J Mol Catal* **1998,** *135(3)* 257 (f) Gallezot, P *Catal Today* **1997,** *37(4)* 405 (g) Ishii, Y *J Mol. Catal* **1997,** *117* 123 (h) Bezant, J C., Besson, M , Gallezot, P *Appl. Catal A-Gen.* **1996,** *135(1)* L7 (i) Rothenberg G , Sasson, Y *Tetrahedron* **1996,** *52(43)* 13641

29 Hendry D G Gould, C W , Schuetzle, D , Syz, M. G , Mayo, F R. *J Org. Chem.* **1976,** *41* 1.

30 Berezin, I V Denisov E. T., Emanuel N M *The oxidation of cyclohexane* London Pergamon. **1966**

31 Schultz, J G. D , Onopchenko, A *J Org Chem* **1980** *45* 3716

32 Tinker, H B *J Catal* **1970,** *19* 237

33 Ito, S , Aihara, K., Matsumoto, M *Tetrahedron Lett* **1984,** *25(35)* 3891

34 Draths, K. M , Frost, J W *J Am Chem Soc* **1993,** *116*, 399.

35 Sato, K , Aoki M , Noyori, R. *Science* 1998, *281* 1646

36 (a) Drago, R. S , Beer R. H , Goldstein, A S *J Am Chem. Soc* **1994,** *116* 2424 (b) Goldstein, A S , Drago R S *Inorg Chem.* **1991,** *30* 4506 (c) Davis S Drago, R. S *J Chem Soc Chem Commun* **1990,** 250 (d) Drago, R S, Davis, S *U S. Patent* **1989,** # 4,885 377 (e) Hamilton, D E , Drago, R S Zombeck A *J Am. Chem Soc* **1987,** *109* 374

37 Riley, R L Ph D dissertation, University of Florida **1989,** 13

38 Sheldrick, G M *SHELXTL5* Bruker-AXS Madison, WI USA **1998.**

39 Prengle, H W Jr , Barona, N *Hydrocarbon Processing* **1970** 106

40 (a) Lyons J E Ellis P E Jr , Myers H K Jr *J Catal* **1995,** *155* 59
(b) Grinstaff M W , Hill M G , Labinger, J A , Gray H B *Science* **1994,** *264* 1311

41 Tanaka, K. *Chemtech.* **1974,** 555

42 Drago R. S , Beer, R. H *Inorg Chim Acta* **1992,** *198-200* 359

43 White R E Coon M J *Annu Rev Biochem* **1980,** *49* 315

44 (a) Barton, D H. R., Doller, D *Acc Chem. Res* **1992,** *25* 504 (b) Barton, D H R. Taylor, D K. *Russ Chem. Bull* **1995,** *44* 575 and references therein. (c) Barton, D H R., Gastiger, M. J., Motherwell, W B *J Chem. Soc Chem. Commun* **1983,** 41

45 Barton, D H R Gastiger, M J Motherwell, W B *J Chem. Soc Chem Commun.* **1983,** 731

46 Balavoine G Barton, D H R , Boivin, J , Lecoupanec, P , Lelandais, P *New J Chem* **1989,** *13* 691

47 Balavoine, G , Barton, D H R. Boivin, J , Gref, A., Ozbalik, N., Riviere H *Tetrahedron Lett* **1986,** *27* 2849

48 Barton D H R. Halley F , Ozbalik N. Young E Balavoine G , Gref, A Boivin J *New J Chem* **1989,** *13* 177

49 Schuchardt, U Krahembul, C E. Z., Carvalho W A. *New J Chem.* **1991,** *15* 955

50 (a) Tung, H.-C., Kang, C., Sawyer, D. T. *J. Am. Chem. Soc.* **1992,** *114* 3445 (b) Sawyer, D. T., Sobkowiak, A., Matsushita, T. *Acc. Chem. Res.* **1996,** *29* 409 (c) Sheu, C. & Sawyer, D. T. *J. Am. Chem. Soc.* **1990,** *112* 8212 (d) Sheu, C., Sobkowiak, A., Jeon, S. & Sawyer, D. T. *J. Am. Chem. Soc.* **1990,** *112* 879

51 Abboud, K. A., Xu, C., Drago, R. S. *Acta Crystallogr.* **1998,** *C54* 1270.

52. (a) Laine, P., Gourdon, A., Launay, J.-P. *Inorg. Chem.* **1995,** *34* 5129 (b) Laine, P., Gourdon, A., Launay, J.-P. *Inorg. Chem.* **1995,** *34* 5138 (c) Laine, P., Gourdon, A., Launay, J.-P., Tuchagues, J.-P. *Inorg. Chem.* **1995,** *34* 5150 (d) Laine, P., Gourdon, A. & Launay, J.-P. *Inorg. Chem.* **1995,** *34* 5156 (e) Hseu, J. F., Chen, J. J., Wei, H. H., Cheng, M. C., Wang, Y., Yan, Y. D. *Inorg. Chem. Acta* **1991,** *184* 1 (f) Thich, J. A., Ou, C. C., Powers, D., Wasiliou, B., Mastropaolo, D., Potenza, J. A., Schugar, H. J. *J. Am. Chem. Soc.* **1976,** *98* 1425

53. Sheldrick, G. M. *SHELXTL. Structure Determination Programs* **1995,** Version 5. Siemens Analytical X-ray Instruments Inc., Madison, WI, USA.

54 (a) Marsh, R. E. *Acta Crystallogr.* **1993,** *C49* 643 (b) Cousson, A., Nectoux, F. *Acta Crystallogr.* **1992,** *C48* 1354

55 (a) Bailey, G. F., Karp, S. & Sacks, L. E. *J. Bacteriol.* **1965,** *89* 984 (b) Setlow, B. & Setlow, P. *Appl. Environ. Microbiol.* **1993,** *59* 640 (c) Waterbury, L. D., Serrato, C. & Martinez, G. R. *Proc. West Pharmac. Soc.* **1989,** *32* 9

56 (a) Morimoto, I. & Tanaka, S. *Anal. Chem.* **1963,** *35* 141 (b) Kanai, Y. *Analyst (London)* **1990,** *115* 809

57 (a) Lee, S.-K., Fox, B. G., Froland, W. A., Lipscomb, J. D., Munck, E. *J. Am. Chem. Soc.* **1993,** *115* 6450 (b) Liu, K. E., Valentine, A. M., Wang, D., Huynh, B. H., Edmondson, D. E., Salifoglou, A., Lippard, S. J. *J. Am. Chem. Soc.* **1995,** *117* 174, and references therein

58 (a) Barton, D. H. R. *Chem. Soc. Rev.* **1996,** 237 (b) Barton, D. H. R., Hu, B., Taylor, D. K., Wahl, R. U. R. *J. Chem. Soc., Perkin Trans. 2* **1996,** 1031

59 Cotton, F. A., Wilkinson, G. *Advanced inorganic chemistry* 5th ed., New York. Wiley **1988**

60 Jorgensen, K. A. *Chem. Rev.* **1989** *89* 431

61 (a) Stinson, S. C. *Chem. Eng. News* **1992** *70(No39)* 46 (b) Nugent, W. A., RajanBabu, T. V., Burk, M. J. *Science* **1993,** *259*, 479

62 Henbest, H B *Chem Soc Spec Publ* **1965,** *19* 83

63 (a) Katsuki T , Sharpless, K. B *J Am. Chem. Soc* **1980,** 102, 5974 (b) Rossiter, B E., Katsuki T , Sharpless K B *J Am. Chem Soc.* **1981,** 103, 464 (c) Martin V S , Woodard, S S , Katsuki, T , Yamada, Y , Ikeda, M., Sharpless, K.B *J Am. Chem Soc.* **1981,** 103, 6237

64 Hansonm R M , Sharpless, K *J Org Chem* **1986,** *51*, 1922

65 (a) Finn, M G , Sharpless K B in *Asymmetric synthesis* J D Morrison, ed., New York Academic Press **1986,** *Vol 5* 247 (b) Williams I D., Pedsen, S F , Sharpless, K B., Lippard, S J *J Am. Chem. Soc* **1984,** *106* 6430

66 (a) Jorgensen K A Wheeler R A Hoffmann R. *J Am Chem Soc* **1987,** *109* 3240 (b) Hansonm R M Sharpless K *J Org Chem* **1986,** *51*, 1922

67 Rossiter, B E in *Asymmetric synthesis* J D Morrison, ed , New York Academic Press **1986,** *Vol 5* 193

68 (a) Groves, J T Viski, P *J Org Chem* **1990,** *55*, 3628 (b) Groves J T., Myers. R. S *J Am Chem Soc* **1983,** *105* 5791 (c) Mansuy D Battioni, P, Renaud T -P Guerin P *J Chem Soc Chem Commun* **1985,** 155 (d) O'Malley S Kodadek T *J Am. Chem Soc* **1989** *111* 9116

69 (a) Jacobsen, E N , Zhang W , Muci A R., Ecker J R , and Deng C *J Am Chem Soc* **1991,** *113* 7063 (b) Irie R Noda, K., Ito Y , Matsumoto N. Katsuki T *Tetrahedron Lett* **1990,** *31* 7345 (c) Larrow J F Jacobsen, E N , Gao, Y , Hong, Y., Nie X., Zepp, C. M *J Org Chem* **1994,** *59* 1939

70 (a) Samsel E G Srinivasan K., Kochi, J K *J Am Chem Soc* **1985,** *107* 7606 (b) Srinivasan K Michaud, P , Kochi, J K. *J Am Chem Soc* **1986,** *108* 2309

71 Zhang W , Loebach, L , Wilson, S R., Jacobsen E N *J Am Chem Soc* **1990,** *112*, 2801

72 Hashihayata, T., Ito, Y., Katsuki, T *Tetrahedron* **1997,** *53* 9541

73 Pietikainen, P *Tetrahedron* **1998,** *54* 4319

74 Bougauchi M , Watanabe S , Arai, T , Sasai, H , Shibasaki, M *J Am Chem. Soc* **1997,** *119* 2329

75 Watanabe S Kobayashi Y Arai T Sasai, H., Bougauchi, M., Shibasaki M *Tetrahedron Lett* **1998,** *39* 7353

76 Daikai, K., Kamaura, M., Inanaga, J. *Tetrahedron Lett* **1998**, *39* 7321

77 (a) Tu, Y., Wang, Z.-X., Shi, Y. *J Am Chem. Soc* **1996**, *118*, 9806 (b) Wang, Z.-X., Tu, Y., Frohn, M., Zhang, J-R., Shi, Y. *J Am. Chem. Soc* **1997**, *119* 11224 (c) Wang, Z.-X., Tu, Y., Frohn, M., Shi, Y. *J Org Chem.* **1997**, *62* 2328 (d) Frohn, M., Dalkiewicz, M., Tu, Y., Wang, Z.-X., Shi, Y. *J Org Chem.* **1998**, *63* 2948

78 He, Q-Y., Mei, Z-H., Zhang, Y-M. *J Coord. Chem.* **1990**, *21* 199

79 Lo, K. Ph.D. dissertation, University of Florida **1997**, 70

80 (a) Jones, R. D., Summerville, D. A., Basolo, F. *Chem Rev* **1979**, *79* 139 (b) Titus, S. J. F., Barr, W. M., Taylor, L. T. *Inorg Chim Acta* **1979**, *32* 103

81 Jorgensen, K. A., Schiøtt, B., Larsen, E. *J Chem Research (S)* **1989**, 214

82 (a) Sattari, D., Alipour, E., Shirani, S., and Amighian, J. *J Inorg Biochem* **1992** *45* 115 (b) Dutta, R. L., Ray, R. K. *J Inorg Nucl Chem* **1976** *39* 1848

83 Yang, Y.-C., Baker, J. A., Ward, J. R. *Chem Rev* **1992**, *92* 1729

84 Anslow, W. P., Jr., Karnofsky, D. A., Jager, B. V., Smith, H. W. *J Pharmacol Exp Ther* **1948**, *93* 1

85 Papirmeister, B., Feister, A. J., Robinson, S. I., Ford, R. D. *Medical defense against mustard gas: toxic mechanisms and pharmacological implications* Boca Raton, FL: CRC Press **1991**

86 Harris, J. M., Paley, M. S., Sedaghat-Herati, M. R., McManus, S. P. *J Org Chem* **1985**, *50* 5230

87 Epstein, J., Bauer, V. E., Saxe, M., Demek, M. M. *J Am Chem. Soc* **1956**, *78*, 4068

88 Richardson, G. A. *Development of a Package Decontamination System* EACR-1310-17, Final Report, Contract DAAA15-71-C-0508 **1972**

89 Harvey, S. P., Height, J. J., Szafraniec, L. L., Beaudry, W. T., DeFrank, J. J., Valdes, J. J., Chakrabarty, A. M. *Abstracts of 91st Annu. Meet. Am. Soc Microbiol.* Dallas, TX **1991** Q119

90 (a) Fox, M. A. *Acc Chem Res* **1983**, *16* 314 (b) Gall, R. D., Hill, C. L., Walker, J. E. *J Catal* **1996**, *159* 473

91 Frank, K. Ph.D. dissertation, University of Florida, **1999**

92. (a) Riesenfeld, E. H.; Mau, W. *Ber. Dtsch. Chem. Ges.* **1911,** *44* 3589 (b) Partington, J. P.; Fathallah, A. H. *J. Chem. Soc.* **1950,** 1934

93 Firsova, T. P.; Alatyreva, N. G.; Stasevich, N. N.; Sakk, Z. G. *Zh. Neorg. Khim.* **1978,** *23* 2633

94 Jones, D. P.; Griffith, W. P. *J. Chem. Soc. Dalton Trans.* **1980,** 2526

95 (a) Flanagan, J.; Jones, D. P.; Griffith, W. P.; Skapski, A. C.; West, A. P. *J. Chem. Soc. Chem. Commun.* **1986,** 20 2526 (b) Brovkina, O. V.; Chernyshov, B. N. *Russ. J. Inorg. Chem.* **1989,** *34* 166.

96 Adam, A.; Mehta, M. *Angew. Chem. Int. Ed.* **1998,** *37* 1387

97 (a) Comyns, A. E. *Nature* **1994,** *369*, 609 (b) Hage, R.; Iburg, J. E.; Kerschner, J.; Koek, J. H.; Lempers, E. L. M.; Martens, R. J.; Racherla, U. S.; Russell, S. W.; Swarthoff, T.; van Vliet, M. R. P.; Warnaar, J. B.; van der Wolf, L.; Krijnen, B. *Nature* **1994,** *369*, 637 (c) Drago, R. S. and Robbins, M. H. *J. Catal.* **1997,** *170* 295

98 (a) Zheng, T.-C.; Richardson, D. E. *Tetrahedron Lett.* **1995,** *36(6)* 833 (b) Zheng, T.-C.; Richardson, D. E. *Tetrahedron Lett.* **1995,** *36* 837

99 Song, R.; Sorokin, A.; Bernadou, J.; Meunier, B. *J. Org. Chem.* **1997,** *62(2)* 673

100 Hodges, G. R.; Smith, J. R. L.; Oakes, J. *J. Chem. Soc. Perkin Trans. 2* **1998,** *12* 617

101 (a) Spadaro, J. T.; Isabelle, L.; Renganathan, V. *Environ. Sci. Tecnol.* **1994,** *28* 1398 (b) Tang, W. Z.; Chen, R. Z. *Chemosphere* **1996,** *32* 947

102 (a) Omura, T.; Kayane, Y.; Tezuka, Y. *Dyes Pigm.* **1992,** *20* 227, (b) Omura, T. *Dyes Pigm.* **1993,** *22* 99, **1993,** *23* 179, **1994,** *24* 125, **1994,** *26* 30

103 (a) Haag, W. R.; Mill, T. *Environ. Toxicol. Chem.* **1987,** *16*, 359 (b) Albini, A.; Fasani, E.; Pietra, S. *J. Chem. Soc. Perkin Trans. 2* **1986,** 617

104 Oakes, J.; Gratton, P.; Clark, R.; Wilkes, I. *J. Chem. Soc. Perkin Trans. 2* **1998,** *12* 2569

105 Oakes, J.; Gratton, P. *J. Chem. Soc. Perkin Trans. 2* **1998,** *12* 2563

106 Sen A Kao L-C *J Chem Soc Chem Commun* **1991,** 1242

107 (*a*) Sen A. Lin M., Kao L-C Hutson, A C *J Am Chem. Soc* **1992,** *114* 6385 (b) Labinger J A, Herring, A M Bercaw J E *J Am. Chem. Soc* **1990,** *112* 5628 (c) Sen A Lin M *J Chem Soc Chem Commun* **1992,** 508 (d) Labinger J A Herring A M, Lyon, D K, Luinstra, G A, Bercaw, J E, Horvath, I T, Eller, K *Organometallics* **1993,** *12* 895

108 Robion, A, Cheo S Wang J, Buchanan, R M, Series, J-L., Fish, R H *J Am. Chem Soc* **1995,** *117* 12356

109 (a) Smith, J R. L., Shul'pin, G B *Tetrahedron Lett* **1998,** *39* 4909 (b) Bolm, C, Kadereit, D, Valacchi, M *Synlett* 1997, 687 (c) Zondervan, C, Hage R., Feringa, B L *J Chem. Soc Chem Commun* **1997,** 419

110 Gilbert, B C Kamp N W J, Smith J R L, Oaks, J *J Chem. Soc Perkin Trans 2* 1998, *12* 1841

111 (a) Ellis, S R US Patent 5041142, **1991** (b) Hage R., Favre, T L F, Helm-Rademaker, K Koek H Martens R J, Swarthoff, T Vliet, M. R. P European Patent 0458397A2 **1991** (c) Harriot, S M US Patent 5021187 **1991** (d) Bragg C D Hardy F A US Patent 5002682 **1991** (e) Dolphin D H Nakano T Kirk, T K Wijesekere T P Farrel, R L, Marone T E US Patent 5041142 **1991** (f) Oakes J US Patent 4481129 **1984**

112 Likussar W and Boltz, D F *Anal Chem* **1971,** *43* 1265

113 Byers G W Gross, S and Henrichs, P M *Photochem. & Photobio* **1975,** *23* 37

114 Faure R. Loiseleur H *Acta Cryst* **1972,** *B28* 2733

115 Mittheilung V *Chem Be* **1888,** *21* 1077

116 (*a*) Arulsamy N and Hodgson D J *Inorg Chem* **1994** 33, 4531 (b) Karlin F D and Tyeklar Z Eds *Bioinorganic chemistry of copper* New York Chapman & Hall. **1993** 236

117 Barton, D H R., Hu, B *Pure & Appl Chem.* **1997,** *69* 1941

BIOGRAPHICAL SKETCH

Cheng Xu was born on September 30, 1961 in Hangzhou, China. He graduated from Hangzhou University with a Bachelor of Science degree in chemistry in 1983.

After an appointment in the Department of Pharmacy, Zhejiang Medical University (1983-1987), he attended graduate school in chemistry at Hangzhou University in 1987 working under Professor Zhaoai Ni. In 1990, Cheng received the degree of Master of Science in chemistry.

In 1990, he was employed as a lecturer at Central Laboratory, Hangzhou University. He was in charge of an instrumental analysis center with 20 chemists and a large set of modern instruments.

Cheng enrolled in the doctoral program in the Department of Chemistry at the University of Florida, studying under the guidance of Dr. Russell S. Drago and Dr. David E. Richardson. His research focuses on the activation of hydrogen peroxide and dioxygen for the catalytic oxidation of organic compounds. The author has several scientific publications and patents.

In 1989, Cheng married Hong Wu. The couple has a beautiful daughter Catherine H. Xu (born on September 15, 1997).

After completing of his doctorate, Cheng Xu will begin postdoctoral research at the University of Pennsylvania, Philadelphia, Pennsylvania.

I certify that I have read this study and that in my opinion it conforms to acceptable standards of scholarly presentation and is fully adequate, in scope and quality, as a dissertation for the degree of Doctor of Philosophy.

David E. Richardson, Chairman
Professor of Chemistry

I certify that I have read this study and that in my opinion it conforms to acceptable standards of scholarly presentation and is fully adequate, in scope and quality, as a dissertation for the degree of Doctor of Philosophy.

William R. Dolbier, Jr.
Professor of Chemistry

I certify that I have read this study and that in my opinion it conforms to acceptable standards of scholarly presentation and is fully adequate, in scope and quality, as a dissertation for the degree of Doctor of Philosophy.

Martin T. Vala, Jr.
Professor of Chemistry

I certify that I have read this study and that in my opinion it conforms to acceptable standards of scholarly presentation and is fully adequate, in scope and quality, as a dissertation for the degree of Doctor of Philosophy.

Daniel R. Talham
Associate Professor of Chemistry

I certify that I have read this study and that in my opinion it conforms to acceptable standards of scholarly presentation and is fully adequate in scope and quality as a dissertation for the degree of Doctor of Philosophy

Hai-Ping Cheng
Associate Professor of Physics

This dissertation was submitted to the Graduate Faculty of the Department of Chemistry in the College of Liberal Arts and Sciences and to the Graduate School and was accepted as partial fulfillment of the requirements for the degree of Doctor of Philosophy

August 1999

Dean Graduate School